Available online at www.derpharmachemica.com

ISSN 0975-413X
CODEN (USA): PCHHAX

Der Pharma Chemica, 2016, 8(1):417-440
(http://derpharmachemica.com/archive.html)

A quantum-chemical analysis of the relationships between electronic structure and cytotoxicity, GyrB inhibition, DNA supercoiling inhibition and anti-tubercular activity of a series of quinoline–aminopiperidine hybrid analogues

Andrés Robles-Navarro and Juan S. Gómez-Jeria*

Quantum Pharmacology Unit, Department of Chemistry, Faculty of Sciences, University of Chile. Las Palmeras 3425, Santiago, Chile

---

ABSTRACT

We present here the results of the application of a formal method relating the electronic structure of a series of quinoline–aminopiperidine hybrid analogues with cytotoxicity, GyrB inhibition, DNA supercoiling inhibition and anti-tubercular activity. The electronic structure of all molecules was obtained with fully optimized geometries at the B3LYP/6-31G(d,p) level. A common skeleton for all the molecules composed by 29 atoms was employed for the study. Linear multiple regression analysis was employed to find the relationships between the variation of the values of the biological activity and the variation of the numerical values of local atomic reactivity indices belonging to the common skeleton. For the four biological activities we found statistically significant relationships with the electronic structure. The two dimensional pharmacophores summarizing the findings can be taken as a starting point for the synthesis and testing of new molecules.

Keywords: Quinoline–aminopiperidine hybrid analogues, DFT calculations, cytotoxicity, anti-tubercular activity, GyrB, DNA supercoiling, QSAR, KPG model.

INTRODUCTION

DNA gyrase (topoisomerase II, Gyr or gyrase), is an enzyme relieving tension while double-stranded DNA is being unwound by helicase. DNA gyrase has two A and B subunits forming a functional heterodimer structure. GyrA has a role in the breakage and reunion of the DNA, while GyrB plays a chief role in ATPase activity. The nonexistence of Gyr in the eukaryotic cells makes this enzyme a very appropriate target for the development of new antibiotics. It is known that gyrase is inhibited by the aminocoumarins and quinolones classes of antibiotics. Several groups of molecules have been synthsized and tested against gyrase [1-29]. Recently, Sriram et al. synthesized a group of novel quinoline–aminopiperidine hybrid analogues and tested them for DNA gyrase-B inhibition, DNA supercoiling inhibition, anti-tubercular activity and cytoxicity [30]. No *formal* structure-activity relationships are known for these molecules. The number of molecules and the four biological activities reported make this set suitable for more detailed study. With this aim, we present here the results of a preliminary application of the Klopman-Peradejordi-Gómez model to find relationships between the electronic/molecular structure of the aforementioned molecules and their biological activities.

MATERIALS AND METHODS

The Method

A technique to find physically-based structure-activity relationships is based on the ensuing idea. First, a model to explain a biological activity is proposed. Subsequently, we employ one or more scientifically-based approximations and convert the assumptions of the model into one or more mathematical equations. In this case, and starting from the statistical-mechanical definition of the equilibrium constant, we developed a method relating the electronic structure of drugs to their *in vitro* receptor affinity constant (K). The final result of this procedure is the following system of n linear equations (for n molecules):

$$\log K_i = a + bM_{D_i} + c\log\left[\sigma_{D_i}/(ABC)^{1/2}\right] + \sum_j \left[e_j Q_j + f_j S_j^E + s_j S_j^N\right] +$$
$$+\sum_j \sum_m \left[h_j(m)F_j(m) + x_j(m)S_j^E(m)\right] + \sum_j \sum_{m'} \left[r_j(m')F_j(m') + t_j(m')S_j^N(m')\right] +$$
$$+\sum_j \left[g_j\mu_j + k_j\eta_j + o_j\omega_j + z_j\varsigma_j + w_j Q_j^{\max}\right] \quad (i=1,\ldots,n) \qquad (1)$$

where K_i is the affinity constant, M is the drug's mass, σ its symmetry number, ABC the product of the drug's moments of inertia about the three principal axes of rotation, Q_i is the net charge of atom i, S_i^E and S_i^N are, respectively, the total atomic electrophilic and nucleophilic superdelocalizabilities of Fukui et al., $F_{i,m}$ is the Fukui index (i.e., the electron population) of atom i in occupied (empty) MO (molecular orbital) m (m'). $S_i^E(m)$ is the electrophilic superdelocalizability of atom i in occupied MO m, $S_i^E(m')$ is the nucleophilic superdelocalizability of atom i in empty MO m'. μ_j, η_j, ω_j, ς_j and Q_j^{max} are the local atomic electronic chemical potential of atom j, the local atomic hardness of atom j, the local atomic electrophilicity of atom j, the local atomic softness of atom j and the maximal amount of electronic charge that atom j may accept. These local atomic reactivity indices (LARIs) are expressed in eV like the global ones and not in eV·e as are the projected local reactivity indices coming from Density Functional Theory. This method is called the Klopman-Peradejordi-Gómez approach (KPG) [31-37]. With this technique, very good structure-activity relationships were found for a variety of drugs and receptors ([38-55] and references therein). Throughout year 2012 this method was extended to any biological activity with outstanding results ([46, 56-68] and references therein).

Selection of biological activities

The selected molecules (41) are shown in Fig. 1 and Table 1 (X=O in 1-20 and X=S in 21-41) [30].

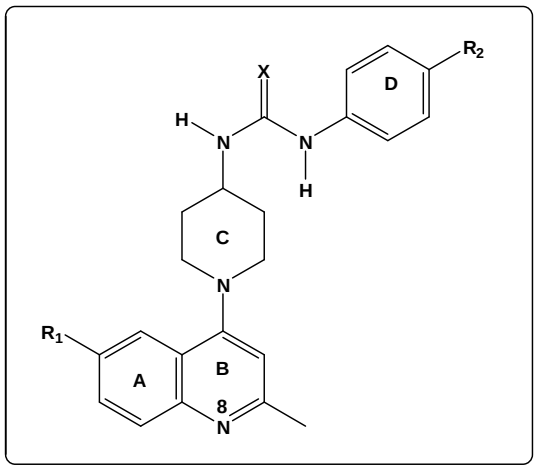

Figure 1. General formula of molecules

Table 1. Selected molecules

Mol.	R_1	R_2		Mol.	R_1	R_2
1	H	H		22	H	Cl
2	H	F		23	H	Me
3	H	NO_2		24	H	OMe
4	H	OMe		25	OMe	H
5	OMe	H		26	OMe	F
6	OMe	F		27	OMe	Cl
7	OMe	Cl		28	OMe	NO_2
8	OMe	NO_2		29	OMe	Me
9	OMe	Me		30	OMe	OMe
10	OMe	OMe		31	F	H
11	F	H		32	F	F
12	F	F		33	F	Cl
13	F	Cl		34	F	NO_2
14	F	NO_2		35	F	OMe
15	F	Me		36	CF_3	H
16	CF_3	H		37	CF_3	F
17	CF_3	F		38	CF_3	Cl
18	CF_3	Cl		39	CF_3	NO_2
19	CF_3	NO_2		40	CF_3	Me
20	CF_3	OMe		41	CF_3	OMe
21	H	H				

The biological activities selected for this study were obtained from a recent publication and are shown in Table 2. They correspond to the *in vitro* inhibition of *Mycobacterium smegmatis* GyrB, the inhibition of *Mycobacterium tuberculosis* DNA supercoiling, the *in vitro* anti-tubercular activity against *Mycobacterium tuberculosis* H37Rv strain (MTB-MIC) and the *in vitro* cytotoxicity in mouse leukemic monocyte macrophage cell line RAW 264.7 cells at a 50 μM concentration (with the MTT assay) [30].

Table 2. Biological activities

Mol.	log(IC_{50}) MS GyrB assay	log(IC_{50}) MTB supercoiling assay	log(MTB-MIC)	log(Cytotoxicity at 50 μM)
1	1.24	0.99	1.41	1.53
2	1.54	1.3	1.53	1.69
3	1.23	1.03	1.19	1.48
4	1.34	1.27	1.51	1.69
5	1.09	0.97	1.51	1.82
6	1.27	1.17	1.41	1.24
7	1.21	1.16	1.24	1.63
8	0.84	0.73	1.17	1.54
9	1.06	0.94	1.19	1.45
10	0.97	0.77	1.1	1.29
11	1.31	0.99	1.52	1.69
12	0.25	-0.11	0.58	1.4
13	1.69	1.47	1.71	1.7
14	0.83	0.33	0.98	1.68
15	1.18	0.95	1.2	1.6
16	1.17	0.92	1.47	1.3
17	1.3	1.07	1.4	1.6
18	1.53	1.24	1.69	1.46
19	1.68	1.35	1.72	1.68
20	1.61	1.3	1.73	1.46
21	1.1	0.97	1.22	1.07
22	1.09	0.91	1.18	1.32
23	0.86	0.42	1.2	1.34
24	1.29	1.13	1.48	1.34
25	0.33	-0.04	0.58	1.62
26	0.94	0.36	1.17	1.47
27	-0.02	-0.21	0.54	1.47
28	0.4	-0.06	0.24	1.4
29	1.05	0.9	0.86	1.65

30	1	0.79	1.2	1.5
31	1.83	1.6	1.8	1.57
32	1.66	1.37	1.8	1.53
33	1.61	1.33	1.5	1.51
34	1.75	1.41	1.8	1.61
35	1.6	1.25	1.5	1.33
36	1.59	1.47	1.55	1.37
37	1.69	1.36	1.82	1.71
38	1.22	0.61	1.49	1.07
39	1.62	0.88	1.71	1.3
40	1.39	0.71	1.5	1.28
41	1.51	1.54	1.83	1.62

CALCULATIONS

We worked assuming that there is a group of common atoms to all the molecules (called common skeleton, CS) that explains almost all the variation of the different biological activities through the variation of the numerical values of their LARIs. This CS is shown in Fig. 2.

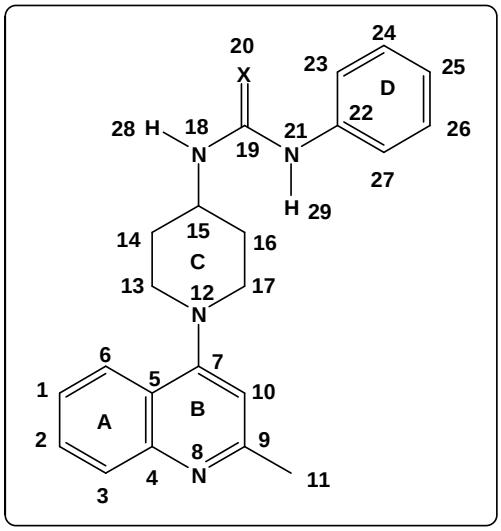

Figure 2. Common skeleton numbering

All the geometries were fully optimized at the DFT B3LYP/6-31G(d,p) level with the Gaussian 03 suite of programs [69]. Using the file of the single point calculations we take out all the required information to calculate the LARIs of Eq. 1 for the atoms composing the CS. The D-Cent-QSAR software was employed [70]. Given that we have not enough experimental biological data to solve the linear system of Eqs. 1, we made use of the usual linear multiple regression analysis techniques to find those indices whose variation explains the variation of the biological activities through the series. The Statistica software was used [71]. In this kind of model statistics is employed as a slave and not as a master.

RESULTS

Results for the *in vitro* cytotoxicity in mouse leukemic monocyte macrophage cell line RAW 264.7 at 50 µM

No good equations were obtained for the whole set (n=41). Therefore, in the first step we carried out a LMRA eliminating the highest experimental value. If no good equation was obtained, we eliminated the second highest experimental value. We followed this iterative procedure until we obtained a statistically significant equation. The basis of this procedure is the hypothesis that, after some high experimental value, the action mechanism possibly changes. The best equation obtained was:

$$\log(\text{Cytotox. at 50 } \mu\text{M}) = 1.21 + 0.18S_5^E(HOMO-1)* + 4.12F_{16}(LUMO+2)* + \\ +0.77F_4(LUMO+2)* + 0.48F_{21}(HOMO)* + 0.05S_{11}^N(LUMO)* \\ -0.001S_{19}^N(LUMO)* - 0.008S_{29}^N(LUMO+1)* + 0.20F_{18}(HOMO-2)* + \\ +0.50S_{15}^E(HOMO-1)* \quad (2)$$

with n=28, R= 0.96, R^2= 0.92, adj-R^2= 0.88, F(9,18)=22.80 (p<0.000001) and a standard error of estimate of 0.05. No outliers were detected and no residuals fall outside the ±2σ limits. Here, $S_5^E(HOMO-1)*$ is the electrophilic superdelocalizability of the second highest occupied MO localized on atom 5, $F_{16}(LUMO+2)*$ is the Fukui index of the third lowest vacant MO localized on atom 16, $F_4(LUMO+2)*$ is the Fukui index of the third lowest vacant MO localized on atom 4, $F_{21}(HOMO)*$ is the Fukui index of the highest occupied MO localized on atom 21, $S_{11}^N(LUMO)*$ is the nucleophilic superdelocalizability of the lowest vacant MO localized on atom 11, $S_{19}^N(LUMO)*$ is the nucleophilic superdelocalizability of the lowest vacant MO localized on atom 19, $S_{29}^N(LUMO+1)*$ is the nucleophilic superdelocalizability of the second lowest vacant MO localized on atom 29, $F_{18}(HOMO-2)*$ is the electrophilic superdelocalizability of the third highest occupied MO localized on atom 18 and $S_{15}^E(HOMO-1)*$ is the electrophilic superdelocalizability of the second highest occupied MO localized on atom 15. Tables 3 and 4 show the beta coefficients and the results of the t-test for significance of coefficients of Eq. 2. Table 5 displays the squared correlation coefficients for the variables appearing in Eq. 2, showing that there are no significant internal correlations. Fig. 3 displays the plot of observed *vs.* calculated $\log(IC_{50})$ values. The associated statistical parameters of Eq. 2 indicate that this equation is statistically significant and that the variation of the numerical value of a group of nine local atomic reactivity indices of atoms of the common skeleton explains about 88% of the variation of log(Cytotox. at 50 μM).

Table 3. Beta coefficients and t-test for significance of coefficients in Eq. 2

Var.	Beta	t(18)	p-level
$S_5^E(HOMO-1)*$	0.56	7.63	<0.000001
$F_{16}(LUMO+2)*$	0.34	4.73	<0.0002
$F_4(LUMO+2)*$	0.61	7.44	<0.000001
$F_{21}(HOMO)*$	0.67	8.08	<0.000001
$S_{11}^N(LUMO)*$	0.29	3.34	<0.004
$S_{19}^N(LUMO)*$	-0.33	-4.18	<0.0006
$S_{29}^N(LUMO+1)*$	-0.29	-3.92	<0.001
$F_{18}(HOMO-2)*$	0.30	3.98	<0.0009
$S_{15}^E(HOMO-1)*$	0.20	2.57	<0.02

Table 4. Matrix of squared correlation coefficients for the variables in Eq. 2

	$S_5^E(HOMO-1)*$	$F_{16}(LUMO+2)*$	$F_4(LUMO+2)*$	$F_{21}(HOMO)*$
$F_{16}(LUMO+2)*$	0.01	1.00		
$F_4(LUMO+2)*$	0.004	0.05	1.00	
$F_{21}(HOMO)*$	0.03	0.02	0.01	1.00
$S_{11}^N(LUMO)*$	0.04	0.03	0.27	0.12
$S_{19}^N(LUMO)*$	0.01	0.04	0.06	0.18
$S_{29}^N(LUMO+1)*$	0.02	0.03	0.02	0.008
$F_{18}(HOMO-2)*$	0.07	0.02	0.03	0.03
$S_{15}^E(HOMO-1)*$	0.05	0.03	0.01	0.10

Table 5. Matrix of squared correlation coefficients for the variables in Eq. 2

	$S_{11}^N(LUMO)*$	$S_{19}^N(LUMO)*$	$S_{29}^N(LUMO+1)*$	$F_{18}(HOMO-2)*$
$S_{11}^N(LUMO)*$	1.00			
$S_{19}^N(LUMO)*$	0.14	1.00		
$S_{29}^N(LUMO+1)*$	0.06	0.03	1.00	
$F_{18}(HOMO-2)*$	0.006	0.001	0.05	1.00
$S_{15}^E(HOMO-1)*$	0.002	0.002	0.006	0.006

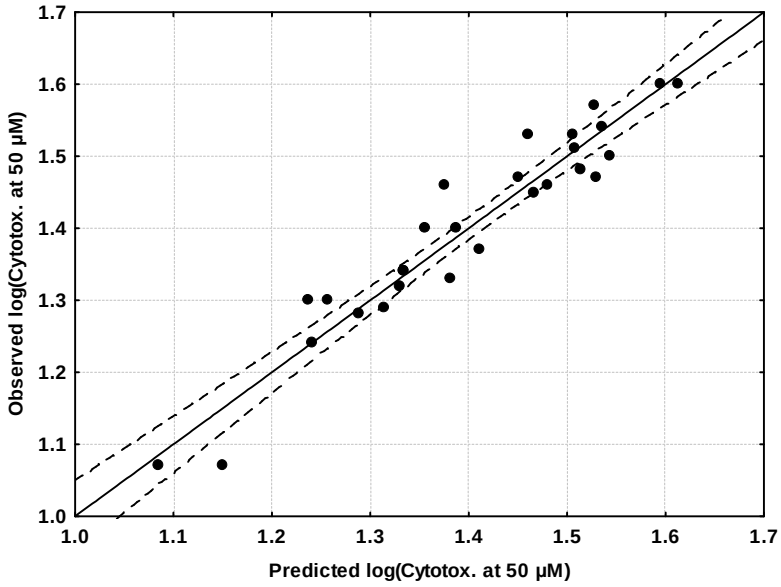

Figure 3. Observed *vs.* calculated $\log(\text{Cytotox. at } 50\ \mu\text{M})$ values (Eq. 2). Dashed lines denote the 95% confidence interval

Results for the *in vitro* inhibition of *Mycobacterium smegmatis* GyrB

Since no good equations were obtained for the whole set (n=41) we proceeded as in the case of cytotoxicity. The best equation is:

$$\log(IC_{50}) = -0.73 + 7.39F_{10}(LUMO+1)* + 0.48S_{21}^E(HOMO-2)* + 1.49F_{23}(LUMO+2)* +$$
$$+0.002S_{27}^N(LUMO)* - 0.03S_4^N(LUMO+1)* - 1.07S_{16}^E(HOMO-2)* -$$
$$-0.13S_{18}^E(HOMO-1)* + 0.45F_{23}(LUMO+1)* - 0.31F_{12}(HOMO)* \quad (3)$$

with n=31, R= 0.97, R^2= 0.94, adj-R^2= 0.92, F(9,21)=37.66 (p<0.000001) and a standard error of estimate of 0.11. No outliers were detected and no residuals fall outside the ±2σ limits. Here, $F_{10}(LUMO+1)*$ is the Fukui index of the second lowest vacant MO localized on atom 10, $S^E_{21}(HOMO-2)*$ is the electrophilic superdelocalizability of the third highest occupied MO localized on atom 21, $F_{23}(LUMO+2)*$ is the Fukui index of the third lowest vacant MO localized on atom 23, $S^N_{27}(LUMO)*$ is the nucleophilic superdelocalizability of the lowest empty MO localized on atom 27, $S^N_4(LUMO+1)*$ is the nucleophilic superdelocalizability of the second lowest vacant MO localized on atom 4, $S^E_{16}(HOMO-2)*$ is the electrophilic superdelocalizability of the third highest occupied MO localized on atom 16, $S^E_{18}(HOMO-1)*$ is the electrophilic superdelocalizability of the second highest occupied MO localized on atom 18, $F_{23}(LUMO+1)*$ is the Fukui index of the second lowest vacant MO localized on atom 23 and $F_{12}(HOMO)*$ is the Fukui index of the highest occupied MO localized on atom 12.

Table 6. Beta coefficients and t-test for significance of coefficients in Eq. 3

Var.	Beta	t(21)	p-level
$F_{10}(LUMO+1)*$	1.05	14.98	<0.000001
$S^E_{21}(HOMO-2)*$	0.43	5.98	<0.000006
$F_{23}(LUMO+2)*$	0.41	5.21	<0.00004
$S^N_{27}(LUMO)*$	0.45	6.96	<0.000001
$S^N_4(LUMO+1)*$	-0.55	-6.78	<0.000001
$S^E_{16}(HOMO-2)*$	-0.21	-3.19	<0.004
$S^E_{18}(HOMO-1)*$	-0.26	-4.16	<0.0004
$F_{23}(LUMO+1)*$	0.18	2.94	<0.008
$F_{12}(HOMO)*$	-0.18	-2.63	<0.02

Table 7. Matrix of squared correlation coefficients for the variables in Eq. 3

	$F_{10}(LUMO+1)*$	$S^E_{21}(HOMO-2)*$	$F_{23}(LUMO+2)*$	$S^N_{27}(LUMO)*$
$S^E_{21}(HOMO-2)*$	0.02	1.00		
$F_{23}(LUMO+2)*$	0.34	0.004	1.00	
$S^N_{27}(LUMO)*$	0.001	0.05	0.08	1.00
$S^N_4(LUMO+1)*$	0.16	0.04	0.38	0.18
$S^E_{16}(HOMO-2)*$	0.00	0.04	0.01	0.04
$S^E_{18}(HOMO-1)*$	0.005	0.01	0.01	0.01
$F_{23}(LUMO+1)*$	0.01	0.07	0.04	0.004
$F_{12}(HOMO)*$	0.04	0.29	0.03	0.04

Table 6 shows the beta coefficients and the results of the t-test for significance of coefficients of Eq. 3. Tables 7 and 8 display the squared correlation coefficients for the variables appearing in Eq. 3, showing that there are no

significant internal correlations. Fig. 4 displays the plot of observed *vs.* calculated $\log(IC_{50})$ values. The associated statistical parameters of Eq. 3 indicate that this equation is statistically significant and that the variation of the numerical value of a group of nine local atomic reactivity indices of atoms of the common skeleton explains about 92% of the variation of this biological activity.

Table 8. Matrix of squared correlation coefficients for the variables in Eq. 3

	$S_4^N(LUMO+1)^*$	$S_{16}^E(HOMO-2)^*$	$S_{18}^E(HOMO-1)^*$	$F_{23}(LUMO+1)^*$
$S_4^N(LUMO+1)^*$	1.00			
$S_{16}^E(HOMO-2)^*$	0.07	1.00		
$S_{18}^E(HOMO-1)^*$	0.07	0.06	1.00	
$F_{23}(LUMO+1)^*$	0.04	0.08	0.06	1.00
$F_{12}(HOMO)^*$	0.04	0.01	0.02	0.01

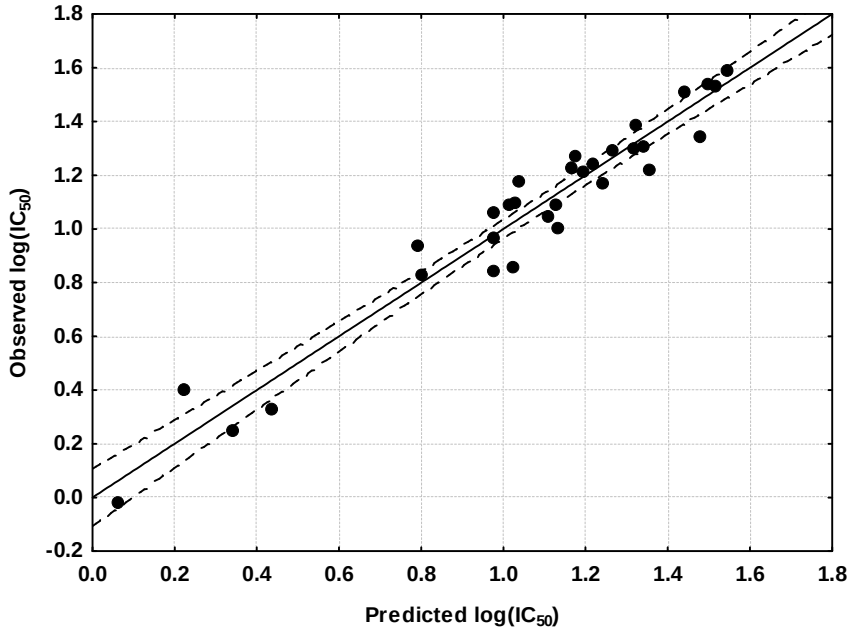

Figure 4. Observed *vs.* calculated $\log(IC_{50})$ values (Eq. 3). Dashed lines denote the 95% confidence interval

Results for the *in vitro* anti-tubercular activity against *Mycobacterium tuberculosis* H37Rv strain (MTB-MIC)
After finding and eliminating three outliers, we obtained the following equation:

$$\log(MTB-MIC) = 2.53+0.21S_{10}^N(LUMO)^*+0.69F_{29}(LUMO+1)^*-0.002S_{23}^N(LUMO+1)^*+$$
$$+0.001S_{26}^N(LUMO+1)^*-0.39S_{14}^N(LUMO)^*+2.56S_{14}^E(HOMO-1)^*-0.78S_{19}^E(HOMO-2)^*+ \quad (4)$$
$$+1.74S_{29}^E(HOMO-1)^*+1.15S_{14}^E(HOMO-2)^*+0.29F_{27}(HOMO-2)^*$$

with n=38, R= 0.96, R^2= 0.92, adj-R^2= 0.89, F(10,27)=31.73 ($p<0.000001$) and a standard error of estimate of 0.10. No outliers were detected and no residuals fall outside the ±2σ limits. Here, $S_{10}^N(LUMO)^*$ is the nucleophilic superdelocalizability of the lowest vacant MO localized on atom 10, $F_{29}(LUMO+1)^*$ is the Fukui index of the second lowest vacant MO localized on atom 29, $S_{23}^N(LUMO+1)^*$ is the nucleophilic superdelocalizability of the

second vacant MO localized on atom 23, $S_{26}^{N}(LUMO+1)*$ is the nucleophilic superdelocalizability of the second lowest vacant MO localized on atom 26, $S_{14}^{N}(LUMO)*$ is the nucleophilic superdelocalizability of the lowest vacant MO localized on atom 14, $S_{14}^{E}(HOMO-1)*$ is the electrophilic superdelocalizability of the second highest occupied MO localized on atom 14, $S_{19}^{E}(HOMO-2)*$ is the electrophilic superdelocalizability of the third highest occupied MO localized on atom 19, $S_{29}^{E}(HOMO-1)*$ is the electrophilic superdelocalizability of the second highest occupied MO localized on atom 29, $S_{14}^{E}(HOMO-2)*$ is the electrophilic superdelocalizability of the third highest occupied MO localized on atom 14 and $F_{27}(HOMO-2)*$ is the Fukui index of the third highest occupied MO localized on atom 27. Table 9 shows the beta coefficients and the results of the t-test for significance of coefficients of Eq. 4.

Table 9. Beta coefficients and t-test for significance of coefficients in Eq. 4

Var.	Beta	t(27)	*p*-level
$S_{10}^{N}(LUMO)*$	0.80	11.54	<0.000001
$F_{29}(LUMO+1)*$	0.49	7.96	<0.000001
$S_{23}^{N}(LUMO+1)*$	-0.42	-6.54	<0.000001
$S_{26}^{N}(LUMO+1)*$	0.24	4.08	<0.0004
$S_{14}^{N}(LUMO)*$	-0.58	-6.99	<0.000001
$S_{14}^{E}(HOMO-1)*$	0.38	5.13	<0.00002
$S_{19}^{E}(HOMO-2)*$	-0.27	-4.57	<0.0001
$S_{29}^{E}(HOMO-1)*$	0.22	3.86	<0.0006
$S_{14}^{E}(HOMO-2)*$	0.22	3.46	<0.002
$F_{27}(HOMO-2)*$	0.18	2.71	<0.01

Table 10. Matrix of squared correlation coefficients for the variables in Eq. 4

	$S_{10}^{N}(LUMO)*$	$F_{29}(LUMO+1)*$	$S_{23}^{N}(LUMO+1)*$	$S_{26}^{N}(LUMO+1)*$	$S_{14}^{N}(LUMO)*$
$F_{29}(LUMO+1)*$	0.06	1.00			
$S_{23}^{N}(LUMO+1)*$	0.06	0.008	1.00		
$S_{26}^{N}(LUMO+1)*$	0.006	0.008	0.08	1.00	
$S_{14}^{N}(LUMO)*$	0.02	0.06	0.004	0.005	1.00
$S_{14}^{E}(HOMO-1)*$	0.05	0.03	0.002	0.005	0.28
$S_{19}^{E}(HOMO-2)*$	0.02	0.02	0.02	0.003	0.01
$S_{29}^{E}(HOMO-1)*$	0.02	0.01	0.003	0.02	0.01
$S_{14}^{E}(HOMO-2)*$	0.04	0.07	0.12	0.008	0.02
$F_{27}(HOMO-2)*$	0.01	0.01	0.02	0.01	0.24

Tables 10 and 11 display the squared correlation coefficients for the variables appearing in Eq. 4, showing that there are no significant internal correlations. Fig. 5 displays the plot of observed *vs.* calculated $\log(\mathrm{IC}_{50})$ values. The associated statistical parameters of Eq. 4 indicate that this equation is statistically significant and that the variation of the numerical value of a group of ten local atomic reactivity indices of atoms of the common skeleton explains about 89% of the variation of log(MTB-MIC).

Table 11. Matrix of squared correlation coefficients for the variables in Eq. 4

	$S_{14}^{E}(HOMO-1)^*$	$S_{19}^{E}(HOMO-2)^*$	$S_{29}^{E}(HOMO-1)^*$	$S_{14}^{E}(HOMO-2)^*$
$S_{14}^{E}(HOMO-1)^*$	1.00			
$S_{19}^{E}(HOMO-2)^*$	0.02	1.00		
$S_{29}^{E}(HOMO-1)^*$	0.008	0.04	1.00	
$S_{14}^{E}(HOMO-2)^*$	0.001	0.008	0.04	1.00
$F_{27}(HOMO-2)^*$	0.01	0.004	0.002	0.001

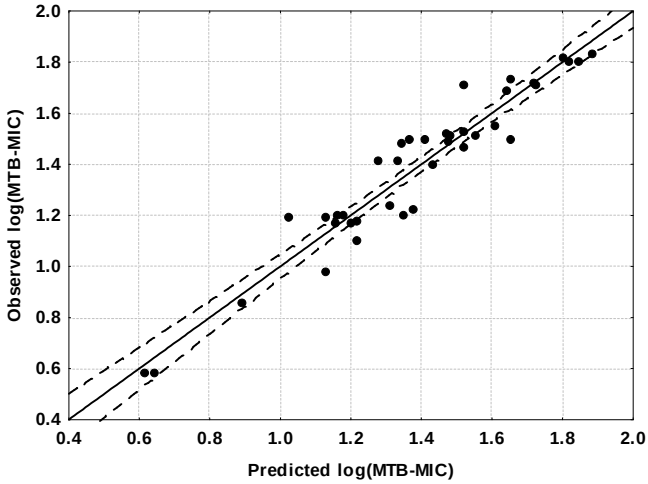

Figure 5. Observed *vs.* calculated $\log(MTB-MC)$ values (Eq. 4). Dashed lines denote the 95% confidence interval

Results for the inhibition of *Mycobacterium tuberculosis* DNA supercoiling

Employing the same technique used for cytotoxicity, we found the following equation:

$$\log(IC_{50}) = 2.02 - 3.03F_2(HOMO)^* + 0.79F_{29}(LUMO+1)^* + 0.44S_{25}^{E}(HOMO-1)^* + \\ + 6.46S_{14}^{E}(HOMO-1)^* + 0.10S_{8}^{E}(HOMO-1)^* - 2.39S_{15}^{E}(HOMO)^* - 0.62F_{23}(LUMO)^* - \\ - 0.28S_{14}^{N}(LUMO)^* - 0.001S_{25}^{N}(LUMO+1)^* + 0.15S_{10}^{E}(HOMO-2)^* + 0.36F_{27}(LUMO+1)^* \quad (5)$$

with n=37, R= 0.97, R^2= 0.94, adj-R^2= 0.92, F(11,25)=38.39 ($p<0.000001$) and a standard error of estimate of 0.12. No outliers were detected and no residuals fall outside the ±2σ limits. Here, $F_2(HOMO)^*$ is the Fukui index of the highest occupied MO localized on atom 2, $F_{29}(LUMO+1)^*$ is the Fukui index of the second lowest vacant MO localized on atom 29, $S_{25}^{E}(HOMO-1)^*$ is the electrophilic superdelocalizability of the second highest occupied MO localized on atom 25, $S_{14}^{E}(HOMO-1)^*$ is the electrophilic superdelocalizability of the second highest occupied MO localized on atom 14, $S_{8}^{E}(HOMO-1)^*$ is the electrophilic superdelocalizability of the

second highest occupied MO localized on atom 8, $S_{15}^{E}(HOMO)*$ is the electrophilic superdelocalizability of the highest occupied MO localized on atom 15, $F_{23}(LUMO)*$ is the Fukui index of the lowest vacant MO localized on atom 23, $S_{14}^{N}(LUMO)*$ is the nucleophilic superdelocalizability of the lowest vacant MO localized on atom 14, $S_{25}^{N}(LUMO+1)*$ is the nucleophilic superdelocalizability of the second lowest vacant MO localized on atom 25, $S_{10}^{E}(HOMO-2)*$ is the electrophilic superdelocalizability of the third highest occupied MO localized on atom 10 and $F_{27}(LUMO+1)*$ is the Fukui index of the second lowest vacant MO localized on atom 27. Table 12 shows the beta coefficients and the results of the t-test for significance of coefficients of Eq. 5. Tables 13 and 14 display the squared correlation coefficients for the variables appearing in Eq. 5, showing that there are no significant internal correlations. Fig. 6 displays the plot of observed *vs.* calculated $\log(\mathrm{IC}_{50})$ values. The associated statistical parameters of Eq. 5 indicate that this equation is statistically significant and that the variation of the numerical value of a group of eleven local atomic reactivity indices of atoms of the common skeleton explains about 89% of the variation of $\log(\mathrm{IC}_{50})$.

Table 12. Beta coefficients and t-test for significance of coefficients in Eq. 5

Var.	Beta	t(25)	p-level
$F_{2}(HOMO)*$	-0.62	-11.03	<0.000001
$F_{29}(LUMO+1)*$	0.39	7.40	<0.000001
$S_{25}^{E}(HOMO-1)*$	0.48	8.23	<0.000001
$S_{14}^{E}(HOMO-1)*$	0.52	9.19	<0.000001
$S_{8}^{E}(HOMO-1)*$	0.16	2.95	<0.007
$S_{15}^{E}(HOMO)*$	-0.25	-4.32	<0.0002
$F_{23}(LUMO)*$	-0.26	-4.54	<0.0001
$S_{14}^{N}(LUMO)*$	-0.26	-4.34	<0.0002
$S_{25}^{N}(LUMO+1)*$	-0.22	-4.28	<0.0002
$S_{10}^{E}(HOMO-2)*$	0.20	3.40	<0.002
$F_{27}(LUMO+1)*$	0.15	2.87	<0.008

Table 13. Matrix of squared correlation coefficients for the variables in Eq. 5

	$F_{2}(HOMO)*$	$F_{29}(LUMO+1)*$	$S_{25}^{E}(HOMO-1)*$	$S_{14}^{E}(HOMO-1)*$	$S_{8}^{E}(HOMO-1)*$
$F_{29}(LUMO+1)*$	0.05	1.00			
$S_{25}^{E}(HOMO-1)*$	0.005	0.01	1.00		
$S_{14}^{E}(HOMO-1)*$	0.05	0.004	0.08	1.00	
$S_{8}^{E}(HOMO-1)*$	0.003	0.004	0.0001	0.002	1.00
$S_{15}^{E}(HOMO)*$	0.03	0.008	0.04	0.09	0.0004
$F_{23}(LUMO)*$	0.04	0.0001	0.15	0.03	0.01
$S_{14}^{N}(LUMO)*$	0.03	0.02	0.11	0.10	0.09
$S_{25}^{N}(LUMO+1)*$	0.03	0.01	0.004	0.0004	0.02
$S_{10}^{E}(HOMO-2)*$	0.003	0.005	0.05	0.001	0.02
$F_{27}(LUMO+1)*$	0.05	0.03	0.0004	0.07	0.006

Table 14. Matrix of squared correlation coefficients for the variables in Eq. 5

	$S_{15}^{E}(HOMO)*$	$F_{23}(LUMO)*$	$S_{14}^{N}(LUMO)*$	$S_{25}^{N}(LUMO+1)*$	$S_{10}^{E}(HOMO-2)*$
$S_{15}^{E}(HOMO)*$	1.00				
$F_{23}(LUMO)*$	0.05	1.00			
$S_{14}^{N}(LUMO)*$	0.004	0.10	1.00		
$S_{25}^{N}(LUMO+1)*$	0.004	0.03	0.002	1.00	
$S_{10}^{E}(HOMO-2)*$	0.11	0.00	0.05	0.04	1.00
$F_{27}(LUMO+1)*$	0.002	0.0001	0.02	0.01	0.02

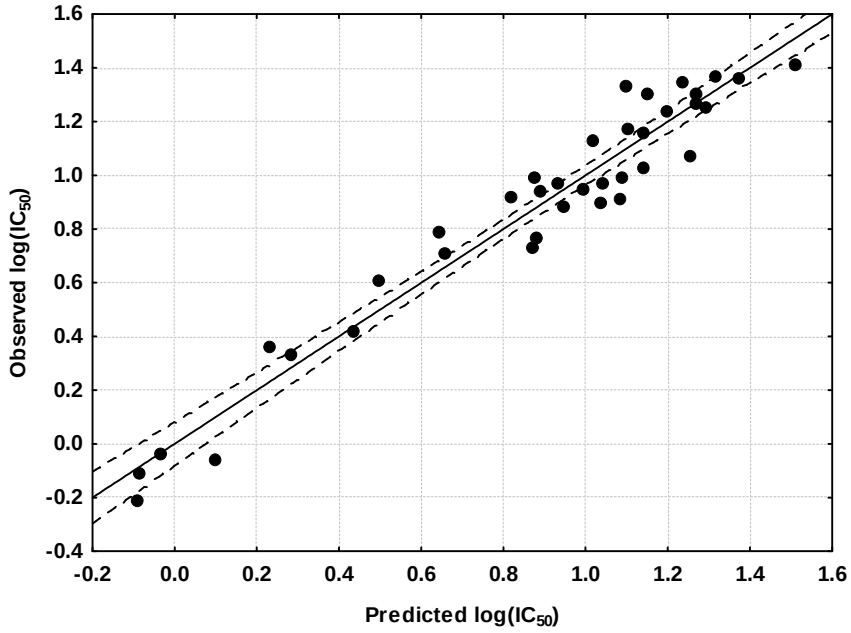

Figure 6. Observed *vs.* calculated $\log(IC_{50})$ values (Eq. 5). Dashed lines denote the 95% confidence interval

Local Molecular Orbitals

Tables 15 to 19 show the local molecular orbital structure of the atoms appearing in Eqs. 2-5 (Reading: molecule's number (HOMO)/ (HOMO-2)*, (HOMO-1)*, (HOMO)*- (LUMO)*, (LUMO+1)*, (LUMO+2)*). Lp denotes a lone pair MO.

Table 15. Local molecular orbital structure of atoms 2, 4, 5 and 8

Mol.	Atom 2 (C)	Atom 4 (C)	Atom 5 (C)	Atom 8 (N)
1 (96)	93π94π96π-97π100π101π	93π94π96π-100π101π103	93π94π96π-97π100π101π	93lp94lp96π-97π100π101π
2 (100)	97π98π100π-101π104π105π	97π98π100π-101π104π105π	97π98π100π-104π105π110π	97lp98lp100π-101π104π105π
3 (107)	105π106π107π-109π111π114π	105π106π107π-111π113π114	105π106π107π-109π111π113π	105lp106lp107π-109π111π113π
4 (104)	101π102π103π-105π106π109π	101π102π103π-105π106π109π	101π102π103π-105π106π109π	100lp101π103π-105π106π109π
5 (104)	99π100π102π-105π106π109π	100σ102π104π-105π106π109π	100σ102π104π-105π106π109π	100lp102π104π-105π106π109π
6 (108)	104π105π106π-109π110π111π	105σ106π108π-109π110π111π	105σ106π108π-109π110π111π	105lp106π108π-109π110π113π
7 (112)	108π109π110π-113π114π115π	109σ110π112π-113π114π115π	109σ110π112π-113π114π115π	109lp110π112π-113π114π117π
8 (115)	111π112π114π-117π119π121π	112σ114σ115π-117π119π121π	112σ114σ115π-117π119π121π	112lp114lp115π-117π119π121π
9 (108)	104π105π106π-109π110π113π	105σ106π108π-109π110π113π	105σ106π108π-109π110π113π	105lp106π108π-109π110π113π
10 (112)	107π108π110π-113π114π117π	108σ110π111π-113π114π117π	108σ110π111π-113π114π117π	108σ110π111π-113π114π117π
11 (100)	94π95π98π-101π102π105π	95σ98π100π-101π102π105π	95σ98π100π-101π102π105π	95lp96lp100π-101π102π105π
12 (104)	100π101π102π-105π106π109π	101σ102π104π-105π106π109π	101π102π104π-105π106π109π	100lp101lp104π-105π106π109π
13 (108)	104π105π106π-109π110π113π	105σ106π108π-109π110π113π	105π106π108π-109π110π113π	104lp105lp108π-109π110π113π
14 (111)	107π108π109π-113π114π115π	108σ109π111π-113π114π115π	108σ109π111π-113π114π115π	107lp108lp111π-113π114π117π
15 (104)	99π100π101π-105π106π109π	101π102π103π-105π106π109π	100π101π103π-105π106π109π	99lp100lp103π-105π106π109π
16 (112)	109π110π112π-113π114π117π	108π109π110π-114π117π124σ	109π110σ112π-114π117π126σ	110lp111π112π-113π114π117π
17 (116)	113π114π116π-117π118π119π	107π113σ114π-118π119π121π	113σ114π116π-117π118π119π	113lp114lp116π-117π118π121π
18 (120)	115π118π119π-121π122π125π	116σ117π118π-122π125π134σ	117π118π119π-121π122π125π	118lp119120π-121π122π125π
19 (123)	120π121π123π-125π126π129π	120σ121π123π-126π129π133π	120σ121π123π-125π126π129π	120lp121lp123π-125π126π129π
20 (120)	117π118π120π-121π122π125π	116σ117π118π-122π125π128π	117π118π120π-121π122π125π	117lp118lp120π-121π122π125π
21 (100)	96π97π98π-101π104π106π	96π97π98π-101π104π106π	95σ96π98π-101π104π106π	96lp97lp98π-101π104π106π
22 (108)	104π105π107π-110π112π115π	103π105π107π-112π115π117σ	105π107π108π-110π112π115π	105lp107π108π-110π112π115π
23 (104)	100π101π103π-105π108π110π	98σ100π103π-105π108π110π	99π100π103π-105π108π110π	100lp103π104π-105π108π110π
24 (108)	103π104π106π-109π110π111π	102σ104π106π-109π110π111π	103π104π106π-109π110π111π	103lp104lp106π-109π113π117lp
25 (108)	102π103π104π-109π111π113π	103σ104π107π-109π111π113π	103σ104π107π-109π111π112π	104π107π108π-109π111π113π
26 (112)	106π107π108π-113π115π116π	107σ108π111π-113π115π116π	107σ108π111π-113π115π116π	108π111π112π-113π115π116π
27 (116)	110π111π112π-117π119π120π	112π115π116π-117π119π120π	112π115π116π-117π119π120π	112π115π116π-117π119π120π
28 (119)	113π114π116π-121π124π125π	114σ116π119π-121π124π125π	114σ116π119π-121π124π125π	114lp116π119π-121π124π125π
29 (112)	107π108π109π-113π115π118π	109π111π112π-113π115π118π	109π111π112π-113π115π118π	109π111π112π-113π115π118π
30 (116)	110π111π112π-117π118π119π	111σ112π114π-117π118π119π	111π112π114π-117π118π119π	111lp112π114π-117π118π119π
31 (104)	97π98π100π-105π107π109π	98σ100π102π-105π107π109π	98σ100π102π-105π107π109π	97lp98lp102π-105π107π109π
32 (108)	102π103π104π-109π111π113π	103σ104π106π-109π111π113π	104π106π107π-109π111π113π	103lp106π107π-109π111π113π
33 (112)	106π107π108π-113π115π118π	108π110π111π-113π115π118π	108π110π111π-113π115π118π	107lp110π111π-113π115π118π
34 (115)	110π111π112π-117π119π120π	111π112π114π-117π119π120π	111π114π115π-117π119π120π	110lp114π115π-117π120π121π
35 (112)	105π107π108π-113π114π117π	107σ108π109π-113π114π117π	107π108π109π-113π114π117π	107lp109π110π-113π114π117π
36 (116)	112π113π115π-117π119π122π	110σ111π112π-119π122π128σ	111π112π115π-119π122π131σ	112lp113π115π-117π119π122π
37 (120)	115π116π119π-121π124π126π	111π115σ116π-124π126π129π	115σ116π119π-121π124π126π	115lp116lp119π-121π124π126π
38 (124)	118π120π122π-125π126π129π	118π119σ120π-126π129π137π	119σ120π122π-125π126π129π	119lp120lp122π-125π126π129π
39 (127)	122π123π125π-129π130π133π	122σ123π125π-130π133π143σ	122σ123π125π-130π133π140σ	122lp123lp125π-129130π133π
40 (120)	115π116π118π-121π123π126π	114σ115σ116π-123π126π135σ	115π116π118π-121π123π126π	116lp118π120π-121π123π126π
41 (124)	119π120π123π-125π127π130π	115π119σ120π-127π130π133π	119σ120π123π-125π127π130π	119lp120lp123π-125π127π130π

Table 16. Local molecular orbital structure of atoms 10, 11, 12 and 14

Mol.	Atom 10 (C)	Atom 11 (C)	Atom 12 (N)	Atom 14 (C)
1 (96)	93π94π96π-97π100π101π	92σ93σ94σ-100σ106σ118σ	93π94π96π-97π101π103lp	91σ94σ96σ-103σ108σ110σ
2 (100)	97π98σ100π-101π104π105π	90σ96σ97σ-104σ110σ124σ	98π99π100π-101π105π110lp	95σ98σ100σ-107σ108σ109σ
3 (107)	105σ106π107π-109π111π114π	96σ103σ106σ-111σ118σ121σ	105π106π107π-109π114π116π	102σ105σ107σ-114σ116σ120σ
4 (104)	101π102π103π-105π106π109π	98σ99σ102σ-106σ114σ125σ	101π102π103π-105π109π111π	101σ102σ103σ-110σ111σ112σ
5 (104)	100σ102π104π-105π106π109π	96σ100σ102σ-106σ115σ117σ	100π102π104π-105π109π113lp	99σ102σ104σ-109σ110σ113σ
6 (108)	105σ106π108π-109π110π111π	100σ105σ106σ-110σ119σ120σ	105π106π108π-109π113π117lp	104σ106σ108σ-113σ114σ117σ
7 (112)	109σ110π112π-113π114π115π	103σ109σ110σ-114σ123σ125σ	109π110π112π-113π117π122lp	108σ110σ112σ-117σ119σ122σ
8 (115)	112σ114π115π-117π119π121π	104σ112σ114σ-119σ127σ128σ	112π114π115π-117π121π125lp	111σ114σ115σ-121σ122σ125σ
9 (108)	105σ106π108π-109π110π113π	104σ105σ106σ-110σ118σ135σ	105π106π108π-109π113π117lp	101σ102σ105σ-113σ114σ117σ
10 (112)	108σ110π111π-113π114π117π	103σ108σ110σ-114σ125σ135σ	108π110π111π-113π117π121lp	109σ110σ111σ-117σ118σ121σ
11 (100)	95σ98π100π-101π102π105π	91σ95σ98σ-102σ109σ120σ	96π98π100π-101π105π109lp	96σ98σ100σ-105σ106σ109σ
12 (104)	101σ102π104π-105π106π109π	100σ101σ102σ-106σ113σ114σ	101π102π104π-105π109π113lp	101σ102σ104σ-109σ111σ118σ
13 (108)	105σ106π108π-109π110π113π	104σ105σ106σ-110σ118σ119σ	105π106π108π-109π113π118lp	105σ106σ108σ-113σ116σ122σ
14 (111)	108σ109π111π-113π114π115π	100σ108σ109σ-114σ122σ131σ	108π109π111π-113π117π119lp	107σ109σ111σ-117σ118σ119σ
15 (104)	101π102π103π-105π106π109π	94σ98σ101σ-106σ113σ127σ	101π102π103π-105π109π111lp	100σ101σ103σ-110σ111σ112σ
16 (112)	110σ111π112π-113π114π117π	102σ107σ109σ-120σ134σ136σ	110π111π112π-113π117π120lp	108σ109σ110σ-117σ118σ121σ
17 (116)	113σ114π116π-117π118π119π	107σ113σ114σ-124σ138σ140σ	112π114π116π-117π121π123π	111σ112σ116σ-121σ126σ127σ
18 (120)	118π119π120π-121π122π125π	110σ116σ118σ-130σ140σ142σ	118π119π120π-121π125π130lp	115σ117σ119σ-125σ127σ131σ
19 (123)	120σ121π123π-125π126π129π	119σ120σ121σ-132σ147σ148σ	119π120π123π-125π129π130lp	112σ118σ120σ-130σ134σ135σ
20 (120)	117π118π120π-121π122π125π	116σ117σ118σ-128σ145σ147σ	115π117π120π-121π125π127lp	113σ117σ118σ-126σ129σ131σ
21 (100)	96π97π98π-101π104π106π	95σ96σ97σ-104σ110σ123σ	96π97π98π-101π106π107lp	95σ97σ98σ-107σ111σ114σ
22 (108)	105π107π108π-110π112π115π	102σ103σ105σ-112σ119σ122σ	105π107π108π-110π115π118lp	103σ104σ107σ-116σ117σ118σ
23 (104)	100π103π104π-105π108π110π	95σ98σ100σ-108σ113σ115σ	101π103π104π-105π110π113lp	99σ101σ103σ-106σ110σ112σ
24 (108)	103σ104π106π-109π110π111π	99σ102σ104σ-118σ119σ130σ	103π104π106π-109π113π116lp	103σ105σ106σ-113σ115σ116σ
25 (108)	103σ104π107π-109π111π113π	99σ103σ104σ-111σ118σ132σ	104π107π108π-109π113π117lp	102σ104σ107σ-113σ115σ117σ
26 (112)	108π111π112π-113π115π116π	103σ107σ108σ-115σ122σ126σ	108π111π112π-113π117π118lp	106σ108σ111σ-117σ119σ121σ
27 (116)	112π115π116π-117π119π120π	107σ111σ112σ-127σ130σ140σ	112π115π116π-117π122π126lp	110σ112σ116σ-122σ124σ126σ
28 (119)	114σ116π119π-121π124π125π	108σ114σ116σ-124σ131σ134σ	114π116π119π-121π125π129lp	113σ116σ119σ-125σ129σ130σ
29 (112)	109π111π112π-113π115π118π	103σ106σ107σ-115σ122σ140σ	109π111π112π-113π118π122lp	104σ107σ108σ-119σ121σ123σ
30 (116)	111σ112π114π-117π118π119π	110σ111σ112σ-126σ136σ142σ	111π112π114π-117π121π125lp	111σ112σ114σ-123σ125σ126σ
31 (104)	98σ100π102π-105π107π109π	95σ98σ100σ-107σ113σ114σ	100π102π103π-105π109π113σ	97σ100σ102σ-109σ111σ113σ
32 (108)	104π106π107π-109π111π113π	102σ103σ104σ-111σ118σ130σ	104π106π107π-109π113π118lp	103σ104σ106σ-116σ119σ120σ
33 (112)	108π110π111π-113π115π118π	106σ107σ108σ-115σ123σ136σ	108π110π111π-113π118π123lp	108σ110σ111σ-120σ121σ124σ
34 (115)	112π114π115π-117π119π120π	103σ110σ111σ-126σ127σ139σ	112π114π115π-117π121π124lp	112σ113σ114σ-125σ127σ128σ
35 (112)	108π109π110π-113π114π117π	105σ107σ108σ-114σ122σ136σ	108π109π110π-113π117π120lp	103σ104σ107σ-117σ123σ124σ
36 (116)	111π112π115π-117π119π122π	106σ110σ111σ-124σ137σ139σ	112π115π116π-117π122π124lp	107σ108σ113σ-118σ122σ125σ
37 (120)	115σ116π119π-121π124π126π	111σ115σ116σ-129σ144σ146σ	114π116π119π-121π126π128lp	114σ117σ119σ-126σ131σ133σ
38 (124)	119σ120π122π-125π126π129π	114σ119σ120σ-134σ136σ145σ	119π120π122π-125π129π134lp	116σ118σ122σ-129σ132σ134σ
39 (127)	122σ123π125π-129π130π133π	121σ122σ123σ-136σ137σ148σ	121π122π125π-129π133π135lp	116σ122σ124σ-138σ139σ144σ
40 (120)	116π118π120π-121π123π126π	114σ115σ116σ-127σ128σ141σ	116π118π120π-121π126π132lp	115σ117σ118σ-130σ132σ139σ
41 (124)	119σ120π123π-125π127π130π	115σ119σ120σ-133σ151σ153σ	118π120π123π-125π130π131lp	115σ116σ121σ-126σ132σ135σ

Table 17. Local molecular orbital structure of atoms 15, 16, 18 and 19

Mol.	Atom 15 (C)	Atom 16 (C)	Atom 18 (N)	Atom 19 (C)
1 (96)	88σ90σ91σ-102σ103σ105σ	87σ88σ94σ-101σ105σ108σ	94π95π96π-99lp102lp105σ	90σ91π95π-99π102π103π
2 (100)	94σ95σ98σ-106σ112σ114σ	94σ95σ98σ-105σ106σ111σ	94π95π98π-103lp106lp107σ	94σ95σ99π-103π106π107π
3 (107)	99σ101σ102σ-112σ113σ115σ	104σ105σ107σ-116σ117σ119σ	101π102π104π-108π112lp115lp	99σ102σ104π-108π112π113σ
4 (104)	93σ97σ99σ-108σ112σ113σ	101σ102σ103σ-109σ111σ113σ	101π102π104π-108π110σ112lp	97σ99σ104π-108π110π111π
5 (104)	95σ97σ98σ-111σ112σ113σ	99σ102σ104σ-110σ111σ114σ	99π101π103π-107π108lp111π	97σ98σ103π-107π108π110σ
6 (108)	98σ101σ103σ-115σ116σ117σ	104σ106σ108σ-114σ115σ118σ	103π104π107π-112π115π116π	101σ103σ107π-112π114σ115π
7 (112)	101σ105σ107σ-120σ122σ124σ	108σ110σ112σ-119σ120σ121σ	107π108π111π-116π120π121π	105σ107σ111π-115π116π119σ
8 (115)	103σ107σ110σ-122σ123σ125σ	113σ114σ115σ-122σ123σ126σ	109π110π113π-116π120π123π	107σ110σ113π-116π120π122σ
9 (108)	99σ101σ102σ-114σ116σ117σ	101σ102σ106σ-115σ117σ122σ	102π103π107π-112π115π116lp	101σ102σ107π-112π114π115π
10 (112)	105σ106σ109σ-119σ120σ122σ	109σ110σ111σ-118σ119σ120σ	108π109π112π-116π119π120lp	106σ109σ112π-116π118σ119π
11 (100)	92σ93σ96σ-107σ108σ110σ	96σ98σ100σ-106σ107σ109σ	96π97π99π-103π107π108lp	93σ96σ99π-103π104π106σ
12 (104)	97σ98σ99σ-111σ112σ114σ	101σ102σ104σ-111σ112σ113σ	100π101π103π-108π112lp113lp	98σ99σ103π-108π110σ111π
13 (108)	101σ102σ103σ-117σ119σ120σ	105σ106σ108σ-116σ117σ118σ	104π105π107π-112π117lp119π	102σ103σ107π-112π115σ116σ
14 (111)	99σ103σ106σ-116σ120σ121σ	109σ110σ111σ-118σ120σ121σ	106π107π110π-112lp116lp118π	103σ106σ110π-112π116π118σ
15 (104)	97σ100σ101σ-111σ112σ114σ	100σ101σ102σ-109σ110σ112σ	101π102π104π-107π108π111π	99σ100σ104π-107π108π111π
16 (112)	103σ105σ108σ-115σ118σ119σ	108σ110σ112σ-121σ122σ124σ	109π110π111π-115lp118lp125π	105σ108σ111π-115π118π119σ
17 (116)	108σ109σ112σ-120σ122σ123σ	109σ111σ112σ-122σ125σ127σ	112π113π115π-120π122lp130lp	111σ112σ115π-120π122π123σ
18 (120)	113σ114σ117σ-128σ129σ131σ	115σ117σ119σ-127σ128σ129σ	117π118π120π-124π128lp129π	114σ117σ120π-123π124π127σ
19 (123)	111σ115σ118σ-128σ131σ133σ	119σ120σ123σ-130σ131σ134σ	119π120π122π-124π128lp131lp	115σ118σ122π-124π128π130σ
20 (120)	113σ117σ118σ-124σ126σ127σ	117σ118σ120σ-125σ126σ131σ	117π118π119π-124lp126lp135lp	117σ118σ119π-123π124π126π
21 (100)	95σ97σ100σ-109σ111σ112σ	92σ95σ97σ-106σ115σ116σ	97π99π100π-102π105π113lp	95π99π100π-102π105π107σ
22 (108)	100σ104σ106σ-109σ113σ118σ	99σ100σ104σ-109σ113σ118σ	105π106σ108π-109lp113lp131lp	106π107π108π-109π113π116σ
23 (104)	96σ101σ102σ-106σ109σ112σ	99σ101σ103σ-111σ112σ114σ	101π102π104π-106lp109lp112lp	101π102π104π-105π106π109π
24 (108)	100σ105σ108σ-111σ114σ117σ	103σ105σ106σ-116σ117σ119σ	105π107π108π-110lp111lp114lp	105π107π108π-110π111π112π
25 (108)	100σ105σ108σ-110σ114σ116σ	104σ105σ107σ-110σ115σ116σ	105π106π108π-110π113lp114lp	105π106π108π-110π113π114π
26 (112)	104σ109σ112σ-117σ120σ121σ	108σ109σ111σ-114σ119σ120σ	109π110π112π-114lp117lp118lp	109π110π112π-114π115π117π
27 (116)	108σ113σ115σ-121σ125σ126σ	112σ113σ116σ-118σ124σ125σ	113π114π115π-118lp121lp125lp	114π115π116π-118π121π124σ
28 (119)	107σ115σ118σ-126σ129σ131σ	116σ117σ119σ-127σ128σ129σ	115π117π118π-120lp122lp123lp	115π117π118π-120π122π123π
29 (112)	104σ109σ112σ-120σ121σ126σ	104σ108σ109σ-121σ126σ131σ	109π110π112π-114lp117lp120lp	110π111π112π-114π117π118π
30 (116)	106σ108σ116σ-124σ125σ127σ	112σ113σ114σ-121σ123σ124σ	113π115π116π-118lp119lp120lp	113π115π116π-118π119π120π
31 (104)	96σ101σ104σ-106σ110σ112σ	101σ102σ103σ-106σ111σ112σ	101π103π104π-106lp110lp112lp	101π103π104π-106π110π111π
32 (108)	100σ105σ108σ-114σ117σ119σ	105σ106σ107σ-113σ115σ116σ	105π107π108π-110lp114lp115lp	105π107π108π-110π112π114π
33 (112)	104σ109σ112σ-117σ122σ123σ	109σ110σ111σ-118σ120σ121σ	110π111π112π-114lp117lp120lp	110π111π112π-114π117π119π
34 (115)	104σ112σ115σ-118σ122σ125σ	112σ114σ115σ-121σ123σ124σ	112π113π115π-116lp118lp119lp	113π114π115π-116π118π119π
35 (112)	103σ104σ112σ-115σ120σ121σ	103σ104σ110σ-119σ120σ121σ	110π111π112π-115lp116lp118lp	110π111π112π-114π115π116π
36 (116)	108σ113σ114σ-118σ121σ123σ	112σ113σ115σ-127σ128σ129σ	113π114π116π-118lp121lp129σ	113π114π116π-118π121π127π
37 (120)	112σ117σ118σ-122σ125σ128σ	111σ112σ117σ-122σ128σ131σ	117π118π120π-122lp125lp134lp	117π118π120π-122π123π125π
38 (124)	116σ121σ124σ-130σ133σ135σ	118σ121σ122σ-127σ131σ132σ	121π123π124π-127lp130lp133lp	121π123π124π-127π130π131π
39 (127)	116σ124σ127σ-138σ139σ140σ	124σ125σ126σ-135σ138σ140σ	124π126π127π-128lp131lp134lp	124π126π127π-128π131π134π
40 (120)	112σ117σ120σ-128σ130σ131σ	117σ118σ120σ-125σ126σ130σ	117π119π120π-122lp125lp128σ	117π119π120π-122π125π127π
41 (124)	116σ121σ122σ-126σ129σ132σ	116σ118σ123σ-130σ135σ136σ	121π122σ124π-126lp128lp129lp	121π122π124π-126π128π129π

Table 18. Local molecular orbital structure of atoms 21, 23, 25 and 26

Mol.	Atom 21 (N)	Atom 23 (C)	Atom 25 (C)	Atom 26 (C)
1 (96)	89σ90σ95π-99π102lp103π	90π91π95π-98π99π102π	87π88π95π-98π99π102π	90π91π95π-98π99π102π
2 (100)	95σ98π99π-103π106π108π	93π98π99π-102π103π108σ	95π98π99π-102π103π106π	93π98π99π-102π103π106π
3 (107)	99σ102σ104π-108π112π115π	101π102π104π-110π112π115σ	99σ102π104π-108π110π112π	101π102π104π-108π110π112π
4 (104)	97σ99σ104π-108π110σ111σ	101π102π104π-107π108π112π	94σ96π104π-107π108π110σ	101π102π104π-107π108π110σ
5 (104)	97σ98σ103π-107π111π112π	98π101π103π-107π108π114σ	92σ95π103π-107π108π111π	98π101π103π-107π108π111π
6 (108)	101σ103σ107π-112π115π116π	102π103π107π-110π111π112π	96σ99π107π-111π112π115π	102π103π107π-110π111π112π
7 (112)	105σ107σ111π-116π120π121π	106π107π111π-114π115π116π	102π104π111π-115π116π118σ	106π107π111π-114π115π116π
8 (115)	107σ110σ113π-116π120π123π	109π110π113π-116π118π120π	106σ110π113π-116π118π120π	109π110π113π-116π118π119π
9 (108)	101σ102σ107π-112π115σ117σ	102π103π107π-111π112π119σ	101σ102π107π-111π112π114π	101σ103107π-111π112π114π
10 (112)	106σ109σ112π-116π119π120π	106π109π112π-115π116π122σ	101σ104π112π-115π116π119π	106π109π112π-115π116π120π
11 (100)	93σ96σ99π-103π107π108π	96π97π99π-103π104π110σ	89σ92π99π-103π104π107π	96π97π99π-103π104π107π
12 (104)	97σ99σ103π-108π111σ112π	98π99π103π-107π108π115σ	93σ96π103π-107π108π110π	98π99π103π-107π108π112π
13 (108)	100π101σ107π-112π116σ117π	102π103π107π-111π112π114σ	99σ100π107π-111π112π114σ	102π103π107π-111π112π114σ
14 (111)	103σ106σ110π-112π116π118σ	105π106π110π-114π115π116π	99π102σ110π-112π115π116π	105π106π110π-112π114π115π
15 (104)	99σ100σ104π-111lp112π115σ	101π102π104π-107π108π118σ	93σ96π104π-107π108π112π	101π102π104π-107π108π112π
16 (112)	105σ111π112π-115π118π127σ	108π111π112π-115π116π118π	105π111π112π-115π116π118π	106π108π111π-115π116π118π
17 (116)	109σ112σ115π-120π122π126π	109σ110π115π-118π119π120π	108π109π115π-119π120π122π	109π110π115π-118π119π120π
18 (120)	117σ119σ120π-124π128π129π	117π119π120π-123π124π126σ	112π119π120π-123π124π126σ	114π117π120π-123π124π126σ
19 (123)	115σ118σ122π-124π128π131π	117π118π122π-124π127π128π	111π114σ122π-124π127π128π	117π118π122π-124π127π128π
20 (120)	117σ118σ119π-124π126π130π	113σ114π119π-123π124π126π	112π113σ119π-123π124π126π	113π114π119π-123π124π126π
21 (100)	97π99π100π-102π105π107σ	95π97π99π-102π103π105π	95π97π99π-102π103π105π	93π95π97π-102π103π105π
22 (108)	106π107π108π-109π113π121σ	104π106π108π-109π111π113π	105π106π108π-109π111π113π	101π104π106π-109π111π113π
23 (104)	102π103π104π-106π109π114σ	101π102π104π-106π107π109π	101π102π104π-106π107π109π	97π101π102π-106π107π109π
24 (108)	105π107π108π-110π111π114π	105π107π108π-111π112π114π	105π107π108π-110π111π112π	105π107π108π-112π114π123σ
25 (108)	105π106π108π-110π113π114π	105π106π108π-110π112π113π	100π105π106π-110π112π113π	102π105π108π-110π112π113π
26 (112)	109π110π112π-114π117π118π	109π110π112π-114π115π116π	109π110π112π-114π116π117π	109π110π112π-114π115π116π
27 (116)	114π115π116π-118π121π137σ	114π115σ116σ-118π119π120π	108π113π114π-118π121π122σ	113π114π115π-118π119π120π
28 (119)	115π117π118π-120π122π123π	115π117π118π-120π122π123π	110σ115π117π-120π122π123π	111σ112π115π-120π122π123π
29 (112)	109π110π112π-114π117π121σ	108π109π110π-114π116π117π	109π110π112π-114π116π117π	108π109π110π-114π116π117π
30 (116)	113π115π116π-118π119π122π	113π115π116π-118π119π120π	113π115π116π-118π119π120π	110π113π115π-118π119π120π
31 (104)	102π103π104π-106π110π126σ	101π103π104π-106π108π110π	96π101π103π-106π108π110π	99π101π104π-106π108π110π
32 (108)	106π107π108π-110π114π116π	105π107π108π-110π112π114π	106π107π108π-110π112π114π	105π107π108π-110π112π114π
33 (112)	110π111π112π-114π117π125π	110π111π112π-114π116π117π	110π111π112π-114π116π117π	105π109π112π-114π116π117π
34 (115)	112π113π115π-116π118π119π	111π112π113π-116π118π119π	111π112π113π-116π118π119π	107π108π112π-116π118π119π
35 (112)	110π111π112π-115π116π118π	110π111π112π-115π116π118π	110π111π112π-115π116π118π	110π111π112π-116π118π123π
36 (116)	113π114π116π-118π121π125π	113π114π116π-118π120π121π	113π114π116π-118π120π121π	108π109π113π-118π120π121π
37 (120)	117π118π120π-122π125π130π	117π118π120π-122π123π125π	117π118π120π-122π123π125π	113π117π118π-122π123π125π
38 (124)	121π123π124π-127π130π139π	121π123π124π-127π128π130π	116π121π123π-127π128π130π	121π123π124π-127π128π130π
39 (127)	124π126π127π-128π131π134π	124π126π127π-128π131π132π	118π124π126π-128π131π132π	119π120π124π-128π132π134π
40 (120)	117π119π120π-122π125π129π	113π117π119π-122π124π125π	112π117π119π-122π124π125π	113π117π119π-122π124π125π
41 (124)	121π122π124π-126π129π134π	121π122π124π-126π128π129π	121π122π124π-126π128π129π	121π122π124π-126π128π129π

Table 19. Local molecular orbital structure of atoms 27 and 29

Mol.	Atom 27 (C)	Atom 29 (H)
1 (96)	90π91π95π-98π99π104σ	70σ78σ90σ-99σ103σ105σ
2 (100)	92σ93π99π-102π103π106σ	65σ76σ99σ-103σ107σ109σ
3 (107)	101π102π104π-108π110π112π	75σ79σ99σ-113σ114σ115σ
4 (104)	101π102π104π-107π108π115σ	74σ83σ97σ-110σ111σ112σ
5 (104)	98π101π103π-107π108π114σ	81σ89σ97σ-109σ110σ111σ
6 (108)	102π103π107π-110π111π112π	87σ88σ101σ-113σ114σ115σ
7 (112)	106π107π111π-114π115π116π	84σ92σ105σ-117σ118σ119σ
8 (115)	109π110π113π-118π119π120π	87σ88σ107σ-119σ121σ122σ
9 (108)	102π103π107π-111π112π119σ	77σ81σ101σ-114σ115σ116σ
10 (112)	106π109π112π-115π116π120π	70σ89σ105σ-117σ118σ119σ
11 (100)	96π97π99π-103π104π110σ	77σ78σ93σ-106σ107σ108σ
12 (104)	98π99π103π-107π108π115σ	81σ84σ97σ-110σ111σ112σ
13 (108)	102π103π107π-111π112π114σ	82σ89σ101σ-114σ115σ116σ
14 (111)	105π106π110π-112π114π115π	85σ87σ103σ-118σ120σ121σ
15 (104)	101π102π104π-107π108π118σ	79σ91σ97σ-110σ111σ112σ
16 (112)	106π108π111π-115π116π121σ	76σ77σ83σ-115σ116σ119σ
17 (116)	109σ110π115π-118π119π120π	74σ76σ90σ-120σ123σ125σ
18 (120)	117π119π120π-123π124π126σ	93σ102σ113σ-126σ127σ129σ
19 (123)	117π118π122π-127π128π135σ	75σ96σ115σ-130σ134σ138σ
20 (120)	113σ114π119π-123π124π130σ	87σ94σ119σ-124σ127σ129σ
21 (100)	95π97π99π-102π103π105π	74σ82σ100σ-102σ108σ109σ
22 (108)	104π106π108π-109π111π113π	69σ71σ72σ-109σ111σ116σ
23 (104)	101π102π104π-106π107π109π	66σ67σ71σ-106σ107σ109σ
24 (108)	105π107π108π-110π111π112π	84σ91σ94σ-110σ111σ115σ
25 (108)	102π105π106π-110π111π112π	75σ93σ96σ-110σ111σ113σ
26 (112)	105π109π110π-114π115π116π	71σ87σ97σ-114σ115σ117σ
27 (116)	109π113π114π-118π119π120π	80σ97σ99σ-119σ121σ122σ
28 (119)	112π115π117π-120π122π123π	98σ99σ101σ-124σ125σ126σ
29 (112)	110π111π112π-114π116π117π	92σ94σ95σ-114σ116σ117σ
30 (116)	113π115π116π-118π119π120π	91σ100σ105σ-118σ119σ123σ
31 (104)	99π101π103π-106π108π110π	74σ89σ90σ-107σ110σ111σ
32 (108)	101π105π107π-110π112π114π	84σ93σ95σ-110σ115σ116σ
33 (112)	109π110π111π-114π116π117π	78σ97σ98σ-114σ117σ118σ
34 (115)	112π113π115π-116π118π119π	80σ88σ97σ-122σ123σ125σ
35 (112)	110π111π112π-115π116π118π	70σ89σ98σ-115σ119σ120σ
36 (116)	113π114π116π-118π120π121π	76σ77σ100σ-118σ120σ121σ
37 (120)	117π118π120π-122π123π125π	77σ80σ97σ-122σ123σ125σ
38 (124)	117π121π123π-127π128π130π	107σ109σ110σ-130σ131σ132σ
39 (127)	120π124π126π-128π131π132π	87σ108σ109σ-131σ134σ135σ
40 (120)	113π117π119π-122π124π125π	74σ76σ80σ-122σ127σ128σ
41 (124)	121π122π124π-126π128π129π	81σ89σ122σ-126σ128σ129σ

DISCUSSION

Discussion of the results for the *in vitro* cytotoxicity in mouse leukemic monocyte macrophage cell line RAW 264.7 at 50 μM

Table 3 shows that the importance of variables in Eq. 2 is $F_{21}(HOMO)^* > F_4(LUMO+2)^* > S_5^E(HOMO-1)^* >> F_{16}(LUMO+2)^* > S_{19}^N(LUMO)^* > F_{18}(HOMO-2)^* > S_{29}^N(LUMO+1)^* > S_{11}^N(LUMO)^* >> S_{15}^E(HOMO-1)^*$. A low cytotoxicity is associated with high negative values for $S_5^E(HOMO-1)^*$ and $S_{15}^E(HOMO-1)^*$; and with low values for $F_{16}(LUMO+2)^*$, $F_{18}(HOMO-2)^*$, $F_4(LUMO+2)^*$ and $F_{21}(HOMO)^*$. The values for the nucleophilic superdelocalizabilities will be discussed below. Atom 5 is a carbon belonging to rings A and B (Fig. 2). Table 15 shows that $(HOMO)_5^*$ is of π nature and that in almost all molecules $(HOMO-1)_5^*$ has the same nature. As a high negative value for $S_5^E(HOMO-1)^*$ is required for low cytotoxicity, we suggest that atom 5 is interacting with an electron deficient center through at least its first two highest occupied local MOs. Atom 16 is a saturated carbon in ring C (Fig. 2). Table 17 shows that all the local MOs are of σ nature. A low cytotoxicity is associated with a low electron population of $(LUMO+2)_{16}^*$. This

may be associated with a repulsive interaction among vacant σ MOs. We tentatively suggest that $(LUMO+1)_{16}^{*}$ and $(LUMO)_{16}^{*}$ could be interacting with occupied σ MOs. These occupied MOs can be localized on the methylene chains of the site. On the other hand, and considering that the local vacant MOs are energetically very far from the molecules' LUMO, it is also possible that this atom be engaged in σ-σ interactions through its local HOMO. If we remember that benzene and cyclohexane have approximately the same boiling point we may understand the importance of σ-σ interactions. We are actually working on a general MO-MO interaction model with the aim to improve this kind of analysis and provide more solid evidence in favor or against one of these two interaction hypothesis. Atom 4 is a carbon belonging to rings A and B and is bonded to atom 5 (Fig. 2). Table 15 shows that most local $(LUMO+2)_4^{*}$ have a π nature. As a low cytotoxicity is associated with low numerical values for $F_4(LUMO+2)^{*}$ we suggest that atom 4 is interacting with an electron rich center through its first two lowest vacant MOs but the third lowest vacant MO seems to be engaged in a repulsive interaction with empty MOs. Atom 21 is a nitrogen belonging to the linker joining rings C and D (Fig. 2). Table 18 shows that $(HOMO)_{21}^{*}$ is a π MO in all molecules. Regarding $(HOMO-1)_{21}^{*}$ and $(HOMO-2)_{21}^{*}$, we have some molecules with a σσ structure and others with ππ structure. Considering that a low cytotoxicity is associated with a low value for the electron population of $(HOMO)_{21}^{*}$ we suggest that this atom is interacting with an electron rich center and that $(HOMO)_{21}^{*}$ could be engaged in a repulsive interaction with one or more occupied MOs. Atom 11 is a methyl substituent in ring B (Fig. 2). Table 16 shows that all local MOs have a σ nature. If $S_{11}^{N}(LUMO)^{*}$ is positive a small value is required for low cytotoxicity. A small positive value is obtained by shifting upwards the $(LUMO)_{11}^{*}$ eigenvalue, making it less reactive. Therefore, we suggest that atom 11 is interacting with σ and/or π vacant MOs. Atom 19 is a carbon belonging to the chain linking rings C and D (Fig. 2). Table 16 shows that $(LUMO)_{19}^{*}$ is of π nature and that sometimes it coincides with the molecular LUMO. Low cytotoxicity is associated with high values of $S_{19}^{N}(LUMO)^{*}$ if the numerical values for this reactivity index are positive. High values are obtained by shifting downwards the energy of the corresponding eigenvalue, making this MO more reactive. Therefore, we suggest that atom 19 is interacting with an electron rich center. Atom 29 is the H atom bonded to N21 (Fig. 2). Table 19 shows that all local MOs are of σ nature.

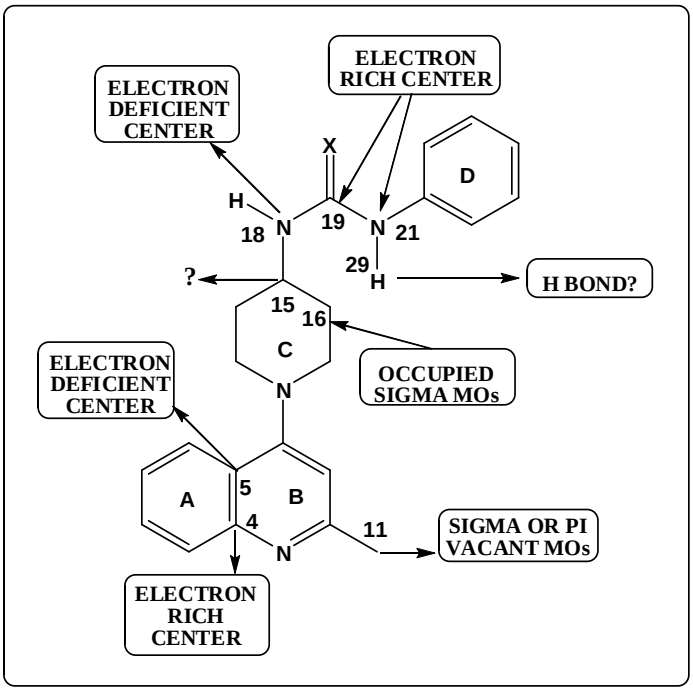

Figure 7. 2D pharmacophore for cytotoxicity at 50 μM

As in the previous case, a low cytotoxicity is associated with high values of $S_{29}^{N}(LUMO+1)^{*}$ if the numerical values of this index are positive. This indicates that this hydrogen atom is interacting with an electron rich center.

This suggests that the N-H group is forming a hydrogen bond with a moiety of the site. This H-bond may be of the classical kind (NH….X, X=O, N, S) or corresponds to N-H….π bonds interactions. Atom 18 is the nitrogen of the chain linking rings C and D (Fig. 2). Table 17 shows that $(HOMO-2)_{18}^{*}$ has π character. A low value for $F_{18}(HOMO-2)*$ can be interpreted as an indication that a low population on this MO is facilitating the action of atom 18 as an electron donor through its first two highest occupied local MOs. Atom 15 will not be discussed because of its high *p* value (see Table 3). All the above suggestion are summarized in the 2D corresponding pharmacophore shown in Fig. 7.

Discussion of the results for the *in vitro* inhibition of *Mycobacterium smegmatis* GyrB.

Table 6 shows that the importance of variables in Eq. 3 is $F_{10}(LUMO+1)*>>S_4^N(LUMO+1)*>S_{27}^N(LUMO)*>S_{21}^E(HOMO-2)*>F_{23}(LUMO+2)*>S_{18}^E(HOMO-1)*>S_{16}^E(HOMO-2)*>F_{23}(LUMO+1)*>F_{12}(HOMO)*$. A high *Mycobacterium smegmatis* GyrB inhibitory capacity is associated with high negative values for $S_{21}^E(HOMO-2)*$, high values for $F_{12}(HOMO)*$, low values for $F_{10}(LUMO+1)*$, $F_{23}(LUMO+1)*$, $F_{23}(LUMO+2)*$ and small negative values for $S_{16}^E(HOMO-2)*$ and $S_{18}^E(HOMO-1)*$. The values for the nucleophilic superdelocalizabilities will be discussed below. Atom 10 is a carbon in ring B (Fig. 2). $(LUMO+1)_{10}^{*}$ has a π nature (Table 16). A low value for $F_{10}(LUMO+1)*$ suggests that atom 10 is interacting with an electron rich center only through its $(LUMO)_{10}^{*}$. Atom 21 is the N atom linking the chain with ring D (Fig. 2). $(HOMO-2)_{21}^{*}$ has a π nature in some molecules and a σ one in others (Table 18). Considering that high negative values of $S_{21}^E(HOMO-2)*$ are associated with a high inhibitory activity, we suggest that atom 21 is interacting with an electron deficient center with at least its first two highest occupied local MOs. In some molecules this interaction is reinforced with the participation of the third highest occupied local π MO. Atom 23 is a carbon in ring D (Fig. 2). $(LUMO+1)_{23}$* has a π nature and $(LUMO+2)_{23}$* has a π nature in some molecules and a σ nature in others (Table 18). A high inhibitory activity is associated with low values for $F_{23}(LUMO+2)*$ and $F_{23}(LUMO+1)*$. This suggests a very specific interaction of $(LUMO)_{23}$* with an electron rich center. Atom 27 is a carbon in ring D (Fig. 2). $(LUMO)_{27}^{*}$ has a π nature (Table 19). If $S_{27}^N(LUMO)*$ is negative, a high inhibitory activity is associated with high negative values for this index. This value is obtained by shifting upwards the associated molecular orbital energy. This, in turn, makes this MO less reactive. The same reasoning holds for positive values of this index. Therefore, we suggest that atom 27 is interacting with an electron deficient center. Atom 4 is a carbon of rings A and B (Fig. 2). $(LUMO+1)_4^{*}$ has a π nature (Table 15). If $S_4^N(LUMO+1)*$ is negative, a high inhibitory activity is associated with small negative values for this index. These small values are obtained by shifting downwards the corresponding eigenvalue making this MO more reactive. Accordingly to this, atom 4 seems to interact with an electron rich center. Atom 16 is a carbon of ring C (Fig. 2). All local MOs are of σ nature (Table 17). Low (negative) values for $S_{16}^E(HOMO-2)*$ are associated with high inhibitory activity. These values are obtained by shifting downwards the corresponding eigenvalue. We suggest that the first two highest occupied local MOs are interacting with an electron deficient center, these interactions being possibly of σ-σ kind. Atom 18 is the N atom linking ring C and the chain (Fig. 2). $(HOMO-1)_{18}^{*}$ is of σ or π nature (Table 17). Low (negative) values of $S_{18}^E(HOMO-1)*$ are associated with high inhibitory activity. This value is obtained by shifting downwards the corresponding eigenvalue and making the MO less reactive. Then, we suggest that atom 18 is interacting with an electron deficient center because $(HOMO-1)_{18}^{*}$ is a π MO (Table 17). Atom 12 is the nitrogen atom of ring C (Fig. 2). $(HOMO)_{12}^{*}$ has π nature (Table 16). High values of $F_{12}(HOMO)*$ are associated with high inhibitory activity. Therefore, we suggest that atom 12 is interacting with an electron deficient center. All the above suggestion are summarized in the 2D corresponding pharmacophore shown in Fig. 8.

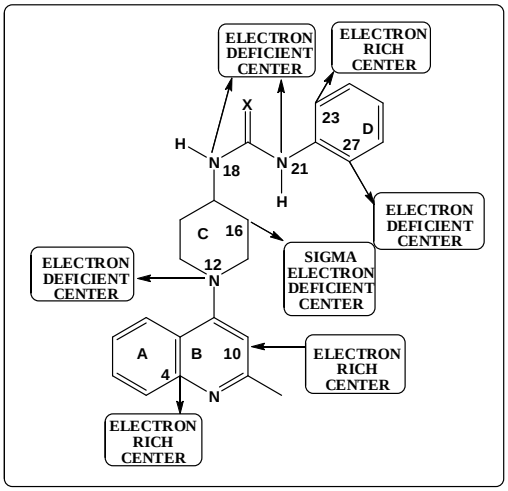

Figure 8. 2D pharmacophore for MS GyrB inhibition

Discussion of the results for the *in vitro* anti-tubercular activity against *Mycobacterium tuberculosis* H37Rv strain (MTB-MIC)

Table 9 shows that the importance of variables in Eq. 4 is $S_{10}^{N}(LUMO)*$> $S_{14}^{N}(LUMO)*$> $F_{29}(LUMO+1)*$> $S_{23}^{N}(LUMO+1)*$> $S_{14}^{E}(HOMO-1)*$>> $S_{19}^{E}(HOMO-2)*$> $S_{26}^{N}(LUMO+1)*$> $S_{29}^{E}(HOMO-1)*$> $S_{14}^{E}(HOMO-2)*$> $F_{27}(HOMO-2)*$. Low MIC values are associated with high (negative) values of $S_{14}^{E}(HOMO-1)*$, $S_{29}^{E}(HOMO-1)*$ and $S_{14}^{E}(HOMO-2)*$, with small (negative) values for $S_{19}^{E}(HOMO-2)*$ and with small (positive) values for $F_{29}(LUMO+1)*$ and $F_{27}(HOMO-2)*$. The values for the nucleophilic superdelocalizabilities will be discussed below. Atom 10 is a carbon of ring B (Fig. 2). $(LUMO)_{10}^{*}$ has a π nature (Table 16). If $S_{10}^{N}(LUMO)*$ is negative, a low MIC value is associated with high negative values. These values are obtained by shifting upwards the corresponding eigenvalue, making this MO less reactive (the same final result is obtained if we consider positive values for $S_{10}^{N}(LUMO)*$). For this reason we suggest that atom 10 is interacting with an electron deficient center. Atom 14 is a carbon of ring C (Fig. 2). All MOs have σ nature (Table 16). A low MIC value is associated with high positive values for $S_{14}^{N}(LUMO)*$, and with low (negative) values for $S_{14}^{E}(HOMO-1)*$ and $S_{14}^{E}(HOMO-2)*$. The appearance of three local atomic reactivity indices could be an indication that ring D is surrounded by a rich molecular environment. To obtain high positive values for $S_{14}^{N}(LUMO)*$, the $(LUMO)_{14}$* energy must be shifted downwards making this MO more reactive. Low negative values for both electrophilic superdelocalizabilities are obtained by shifting downwards the associated eigenvalues, making both MOs less reactive. We can see that the requirements for these three reactivity indices are not contradictory. Therefore, we suggest that atom 14 is interacting with a rich electron center or centers, possibly of hydrophobic nature. Atom 29 is the hydrogen bonded to N21 (Fig. 2). All MOs are of σ nature (Table 19). A low MIC value is associated with small values for $F_{29}(LUMO+1)*$ and with high (negative) values for $S_{29}^{E}(HOMO-1)*$. Small values for $F_{29}(LUMO+1)*$ suggest that this MO could be engaged in a repulsive interaction with one or more vacant MOs. High negative values for $S_{29}^{E}(HOMO-1)*$ indicate that low MIC values are obtained when this MO is more reactive. Therefore, a coherent interpretation suggests that this hydrogen atom could be involved in a hydrogen bond of the N-H….O kind. Atom 23 is a carbon of ring D (Fig. 2). $(LUMO+1)_{23}^{*}$ has a π nature (Table 18). When $S_{23}^{N}(LUMO+1)*$ is positive, low MIC values are associated with high values of this index. These values are obtained by shifting downwards the corresponding eigenvalue and making this MO more reactive. For this reason we suggest that atom 23 is interacting with an electron rich center.

Atom 19 is the carbon of the chain linking rings C and D (Fig. 2). Low MIC values are associated with low (negative) $S_{19}^{E}(HOMO-2)*$ values. $(HOMO-2)_{19}^{*}$ and $(HOMO-1)_{19}^{*}$ have a π nature in some molecules and a σ nature in others (Table 17, see below for comments concerning this fact). $(HOMO)_{19}^{*}$ has a π nature. We suggest that this atom in interacting with an electron deficient center and that the ideal situation is when the first two highest occupied local MOs have a π nature. Atom 26 is a carbon of ring D (Fig. 2). $(LUMO+1)_{26}^{*}$ has a π nature (Table 18). When $S_{26}^{N}(LUMO+1)*$ is positive, low MIC values are associated with small values of this index. These values are obtained by shifting upwards the corresponding eigenvalue, making this MO less reactive. This, in turn, suggests that atom 26 could be interacting with an electron deficient center. It should be noted that, for this interpretation, we have assumed that the $(LUMO)_{26}^{*}$ energy also shifts upwards. Atom 27 is a carbon of ring D and it will not be discussed because of its associated low *p* value (Table 9). All the above suggestion are summarized in the 2D corresponding pharmacophore shown in Fig. 9.

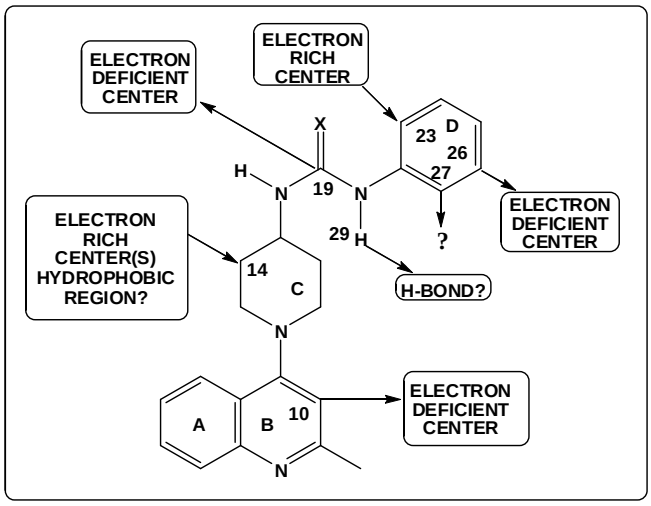

Figure 9. 2D pharmacophore for the minimum inhibitory concentration on *M. tuberculosis* H37Rv strain

Discussion of the results for the inhibition of *Mycobacterium tuberculosis* DNA supercoiling

Table 12 shows that the importance of variables in Eq. 5 is $F_2(HOMO)*>$ $S_{14}^{E}(HOMO-1)*>$ $S_{25}^{E}(HOMO-1)*>$ $F_{29}(LUMO+1)*>>$ $S_{14}^{N}(LUMO)*=$ $F_{23}(LUMO)*>$ $S_{15}^{E}(HOMO)*>$ $S_{25}^{N}(LUMO+1)*>S_{10}^{E}(HOMO-2)*>$ $S_{8}^{E}(HOMO-1)*>F_{27}(LUMO+1)*$. A high inhibitory capacity is associated with high (negative) values of $S_{25}^{E}(HOMO-1)*$, $S_{14}^{E}(HOMO-1)*$, $S_{8}^{E}(HOMO-1)*$ and $S_{10}^{E}(HOMO-2)*$, with high values for $F_2(HOMO)*$ and $F_{23}(LUMO)*$, with small values for $F_{29}(LUMO+1)*$ and $F_{27}(LUMO+1)*$, and with low (negative) values for $S_{15}^{E}(HOMO)*$. The values for the nucleophilic superdelocalizabilities will be discussed below. Atom 2 is a carbon atom of ring A (Fig. 2). $(HOMO)_2^{*}$ has a π nature (Table 15). A high value of $F_2(HOMO)*$ suggests that atom 2 is interacting with an electron deficient center. Atom 29 is the hydrogen atom attached to N21 (Fig. 2). $(LUMO+1)_{29}^{*}$ is a σ MO in all molecules (Table 19). A low value for $F_{29}(LUMO+1)*$ is required for high inhibitory activity. In the ideal situation this MO should have a zero electron population on this atom. This could be an indirect indication that this H atom could serve as a bridge to donate electrons to a more electronegative center that N21. If this is true, then the molecule-site interaction should be of the N-H…O kind. Atom 25 is a carbon of ring D (Fig. 2). $(HOMO-1)_{25}^{*}$ has a π nature (Table 18). High inhibitory activity is associated with high (negative) values of $S_{25}^{E}(HOMO-1)*$. This suggests that atom 25 is interacting with an electron deficient center. On the other hand, if the values of $S_{25}^{N}(LUMO+1)*$ are positive, a high inhibitory activity is associated with high values of this index. This

suggests that atom 25 is interacting with an electron rich center. Considering the *p* values associated to these two indices (Table 12) the interaction of atom 25 with an electron deficient center is more probable, but the possibility of both interactions with different centers should not be ruled out. Atom 14 is a carbon of ring C (Fig. 2). $(HOMO-1)_{14}^{*}$ and $(LUMO)_{14}^{*}$ are σ MOs. A high inhibitory activity is associated with high (negative) values of $S_{14}^{E}(HOMO-1)*$. If the values of $S_{14}^{N}(LUMO)*$ are positive, then a high activity is related to high values of this index. The associated *p* values of these two variables (Table 12) indicate that $S_{14}^{E}(HOMO-1)*$ is more relevant. Therefore, we suggest the interaction of atom 14 with a site possessing vacant σ MOs and, possible, also with another site with occupied σ MOs. If both situations happen it is possible that atom 14 is close to a hydrophobic environment. Atom 8 is a nitrogen in ring B (Fig. 2). $(HOMO-1)_{8}^{*}$ has a π or lp nature (Table 15). A high inhibitory activity is associated with high (negative) values of $S_{8}^{E}(HOMO-1)*$. Therefore we suggest that this atom is interacting with an electron deficient center. The optimal situation should occur if $(HOMO-1)_{8}^{*}$ has a π nature. Atom 15 is a carbon in ring C (Fig. 2). $(HOMO)_{15}^{*}$ is of σ nature (Table 17). A high inhibitory activity is associated to low (negative) values of $S_{15}^{E}(HOMO)*$. This suggests that atom 15 could be interacting with a center having occupied σ MOs. Atom 23 is a carbon in ring D (Fig. 2). $(LUMO)_{23}^{*}$ has a π nature (Table 18). As a high inhibitory activity is associated with high values of this index, we suggest that atom 23 is interacting with an electron rich center. Atom 10 is a carbon in ring B (Fig. 2). $(HOMO-2)_{10}^{*}$ has a π or σ nature (Table 16). A high inhibitory activity is associated with high (negative) values for $S_{10}^{E}(HOMO-2)*$. We suggest that this atom is interacting with an electron deficient center. In some cases it uses the two highest occupied local MOs and in others only the local HOMO*. Atom 27 is a carbon in ring D (Fig. 2). $(LUMO+1)_{27}^{*}$ has a π nature (Table 19). A high inhibitory activity is associated with small values of $F_{27}(LUMO+1)*$. As $(LUMO)_{27}^{*}$ has a small electron population (not shown here) we suggest that this atom is interacting with an electron deficient center. All the above suggestion are summarized in the 2D corresponding pharmacophore shown in Fig. 10.

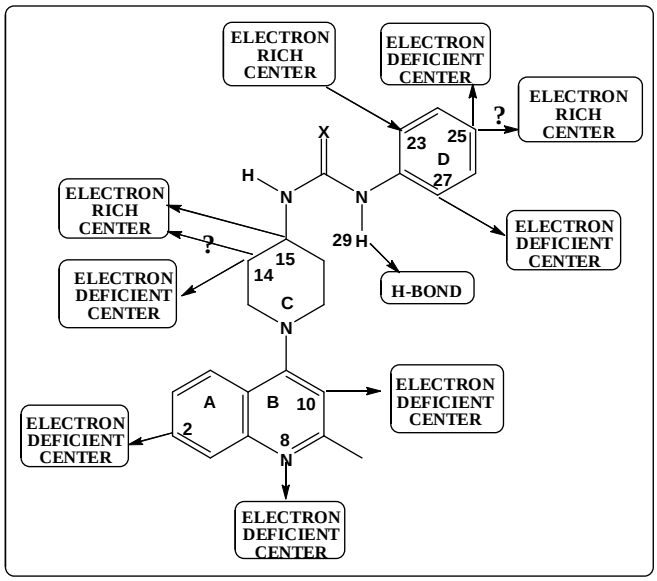

Figure 10. 2D pharmacophore for the inhibition of *Mycobacterium tuberculosis* DNA supercoiling

Some words about the pharmacophores are necessaries. We have presented two-dimensional pharmacophores because we do not know the active conformation. This representation has a weak side. Let us consider for example Fig. 10. We can see that three atoms of ring D interact with electron-rich and/or electron-deficient centers. But these centers are not necessarily separate entities. In fact, they could belong to a six-membered aromatic ring for example. A similar situation may occur in the case of atoms 14 and 15 of ring D. This set of molecules shows a difficulty related to the different natures of a given local molecular orbital (π and σ, π and lp, etc.). We are actually working in a general approach to solve it.

In summary, for the four biological activities we have found statistically significant relationships with the electronic structure. The 2D pharmacophores summarizing these findings can be taken as a starting point for the synthesis and testing of new structures.

REFERENCES

[1] JF Barrett, JI Bernstein, HM Krause, JJ Hilliard, KA Ohemeng, *Analytical Biochemistry*, **1993**, 214, 313-317.
[2] E Goetschi, P Angehrn, H Gmuender, P Hebeisen, H Link, et al., *Pharmacol. Ther.*, **1993**, 60, 367-380.
[3] H Gmünder, P Angehrn, E Götschl, N Nakada, M Stieger, *Pharmacol. Res.*, **1995**, 31, Supplement 1, 135.
[4] D Barrett, H Sasaki, T Kinoshita, A Fujikawa, K Sakane, *Tetrahedron*, **1996**, 52, 8471-8488.
[5] T Lübbers, P Angehrn, H Gmünder, S Herzig, J Kulhanek, *Bioorg. Med. Chem. Lett.*, **2000**, 10, 821-826.
[6] A Tanitame, Y Oyamada, K Ofuji, M Fujimoto, K Suzuki, et al., *Bioorg. Med. Chem.*, **2004**, 12, 5515-5524.
[7] A Tanitame, Y Oyamada, K Ofuji, Y Kyoya, K Suzuki, et al., *Bioorg. Med. Chem. Lett.*, **2004**, 14, 2857-2862.
[8] A Tanitame, Y Oyamada, K Ofuji, K Suzuki, H Ito, et al., *Bioorg. Med. Chem. Lett.*, **2004**, 14, 2863-2866.
[9] M Oblak, SG Grdadolnik, M Kotnik, R Jerala, M Filipič, et al., *Bioorg. Med. Chem. Lett.*, **2005**, 15, 5207-5210.
[10] A Tanitame, Y Oyamada, K Ofuji, H Terauchi, M Kawasaki, et al., *Bioorg. Med. Chem. Lett.*, **2005**, 15, 4299-4303.
[11] M Oblak, SG Grdadolnik, M Kotnik, A Poterszman, RA Atkinson, et al., *Biochem. Biophys. Res. Comm*, **2006**, 349, 1206-1213.
[12] T Lübbers, P Angehrn, H Gmünder, S Herzig, *Bioorg. Med. Chem. Lett.*, **2007**, 17, 4708-4714.
[13] TP Tran, EL Ellsworth, JP Sanchez, BM Watson, MA Stier, et al., *Bioorg. Med. Chem. Lett.*, **2007**, 17, 1312-1320.
[14] SP East, CB White, O Barker, S Barker, J Bennett, et al., *Bioorg. Med. Chem. Lett.*, **2009**, 19, 894-899.
[15] M Brvar, A Perdih, M Oblak, LP Mašič, T Solmajer, *Bioorg. Med. Chem. Lett.*, **2010**, 20, 958-962.
[16] BA Sherer, K Hull, O Green, G Basarab, S Hauck, et al., *Bioorg. Med. Chem. Lett.*, **2011**, 21, 7416-7420.
[17] M Brvar, A Perdih, V Hodnik, M Renko, G Anderluh, et al., *Bioorg. Med. Chem.*, **2012**, 20, 2572-2580.
[18] Z Huang, K Lin, Q You, *Bioorg. Med. Chem. Lett.*, **2013**, 23, 4166-4171.
[19] MJ Mitton-Fry, SJ Brickner, JC Hamel, L Brennan, JM Casavant, et al., *Bioorg. Med. Chem. Lett.*, **2013**, 23, 2955-2961.
[20] LW Tari, M Trzoss, DC Bensen, X Li, Z Chen, et al., *Bioorg. Med. Chem. Lett.*, **2013**, 23, 1529-1536.
[21] M Trzoss, DC Bensen, X Li, Z Chen, T Lam, et al., *Bioorg. Med. Chem. Lett.*, **2013**, 23, 1537-1543.
[22] M Uria-Nickelsen, A Blodgett, H Kamp, A Eakin, B Sherer, et al., *Int. J. Antimicrob. Ag.*, **2013**, 41, 28-35.
[23] J Verghese, T Nguyen, LM Oppegard, LM Seivert, H Hiasa, et al., *Bioorg. Med. Chem. Lett.*, **2013**, 23, 5874-5877.
[24] MI Abdullah, A Mahmood, M Madni, S Masood, M Kashif, *Bioorg. Chem*, **2014**, 54, 31-37.
[25] VU Jeankumar, J Renuka, VK Pulla, V Soni, JP Sridevi, et al., *Int. J. Antimicrob. Ag.*, **2014**, 43, 269-278.
[26] RR Kale, MG Kale, D Waterson, A Raichurkar, SP Hameed, et al., *Bioorg. Med. Chem. Lett.*, **2014**, 24, 870-879.
[27] IA Yule, LG Czaplewski, S Pommier, DT Davies, SK Narramore, et al., *Eur. J. Med. Chem.*, **2014**, 86, 31-38.
[28] MA Azam, J Thathan, S Jubie, *Bioorg. Chem*, **2015**, 62, 41-63.
[29] M Chandran, J Renuka, JP Sridevi, GS Pedgaonkar, V Asmitha, et al., *Int. J. Mycobact.*, **2015**, 4, 104-115.
[30] B Medapi, J Renuka, S Saxena, JP Sridevi, R Medishetti, et al., *Bioorg. Med. Chem.*, **2015**, 23, 2062-2078.
[31] JS Gómez-Jeria, *Canad. Chem. Trans.*, **2013**, 1, 25-55.
[32] JS Gómez-Jeria, *Elements of Molecular Electronic Pharmacology (in Spanish)*, Ediciones Sokar, Santiago de Chile, **2013**.
[33] JS Gómez-Jeria, M Ojeda-Vergara, *J. Chil. Chem. Soc.*, **2003**, 48, 119-124.
[34] JS Gómez-Jeria, "Modeling the Drug-Receptor Interaction in Quantum Pharmacology," in *Molecules in Physics, Chemistry, and Biology*, J. Maruani Ed., vol. 4, pp. 215-231, Springer Netherlands, **1989**.
[35] JS Gómez-Jeria, *Int. J. Quant. Chem.*, **1983**, 23, 1969-1972.
[36] F Peradejordi, AN Martin, A Cammarata, *J. Pharm. Sci.*, **1971**, 60, 576-582.
[37] G Klopman, *J. Am. Chem. Soc.*, **1968**, 90, 223-234.
[38] MS Leal, A Robles-Navarro, JS Gómez-Jeria, *Der Pharm. Lett.*, **2015**, 7, 54-66.
[39] JS Gómez-Jeria, J Valdebenito-Gamboa, *Res. J. Pharmac. Biol. Chem. Sci.*, **2015**, 6, 203-218.
[40] JS Gómez-Jeria, J Valdebenito-Gamboa, *Der Pharma Chem.*, **2015**, 7, 323-347.
[41] JS Gómez-Jeria, J Valdebenito-Gamboa, *Der Pharm. Lett.*, **2015**, 7, 211-219.
[42] JS Gómez-Jeria, A Robles-Navarro, *Res. J. Pharmac. Biol. Chem. Sci.*, **2015**, 6, 1358-1373.

[43] JS Gómez-Jeria, A Robles-Navarro, *Res. J. Pharmac. Biol. Chem. Sci.*, **2015**, 6, 1811-1841.
[44] JS Gómez-Jeria, A Robles-Navarro, *J. Comput. Methods Drug Des.*, **2015**, 5, 15-26.
[45] JS Gómez-Jeria, A Robles-Navarro, *Der Pharma Chem.*, **2015**, 7, 243-269.
[46] JS Gómez-Jeria, A Robles-Navarro, *Res. J. Pharmac. Biol. Chem. Sci.*, **2015**, 6, 1337-1351.
[47] JS Gómez-Jeria, I Reyes-Díaz, J Valdebenito-Gamboa, *J. Comput. Methods Drug Des.*, **2015**, 5, 25-56.
[48] R Solís-Gutiérrez, JS Gómez-Jeria, *Res. J. Pharmac. Biol. Chem. Sci.*, **2014**, 5, 1401-1416.
[49] F Salgado-Valdés, JS Gómez-Jeria, *J. Quant. Chem.*, **2014**, 2014 Article ID 431432, 1-15.
[50] JS Gómez-Jeria, J Valdebenito-Gamboa, *Der Pharma Chem.*, **2014**, 6, 383-406.
[51] JS Gómez-Jeria, J Molina-Hidalgo, *J. Comput. Methods Drug Des.*, **2014**, 4, 1-9.
[52] JS Gómez-Jeria, *Res. J. Pharmac. Biol. Chem. Sci*., **2014**, 5, 780-792.
[53] JS Gómez-Jeria, *Res. J. Pharmac. Biol. Chem. Sci*., **2014**, 5, 2124-2142.
[54] JS Gómez-Jeria, *SOP Trans. Phys. Chem.*, **2014**, 1, 10-28.
[55] JS Gómez-Jeria, *Der Pharm. Lett.*, **2014**, 6., 95-104.
[56] J Valdebenito-Gamboa, JS Gómez-Jeria, *Der Pharma Chem.*, **2015**, 7, 543-555.
[57] JS Gómez-Jeria, J Valdebenito-Gamboa, *Der Pharma Chem.*, **2015**, 7, 103-121.
[58] JS Gómez-Jeria, A Robles-Navarro, *Res. J. Pharmac. Biol. Chem. Sci.*, **2015**, 6, 755-783.
[59] JS Gómez-Jeria, MB Becerra-Ruiz, *Der Pharma Chem.*, **2015**, 7, 362-369.
[60] JS Gómez-Jeria, *Res. J. Pharmac. Biol. Chem. Sci*., **2015**, 6, 688-697.
[61] DI Pino-Ramírez, JS Gómez-Jeria, *Amer. Chem. Sci. J.*, **2014**, 4, 554-575.
[62] D Muñoz-Gacitúa, JS Gómez-Jeria, *J. Comput. Methods Drug Des.*, **2014**, 4, 48-63.
[63] D Muñoz-Gacitúa, JS Gómez-Jeria, *J. Comput. Methods Drug Des.*, **2014**, 4, 33-47.
[64] JS Gómez-Jeria, *J. Comput. Methods Drug Des.*, **2014**, 4, 38-47.
[65] JS Gómez-Jeria, *Der Pharma Chem.*, **2014**, 6, 64-77.
[66] JS Gómez-Jeria, *Brit. Microbiol. Res. J.*, **2014**, 4, 968-987.
[67] JS Gómez-Jeria, *Int. Res. J. Pure App. Chem.*, **2014**, 4, 270-291.
[68] F Gatica-Díaz, JS Gómez-Jeria, *J. Comput. Methods Drug Des.*, **2014**, 4, 79-120.
[69] MJ Frisch, GW Trucks, HB Schlegel, GE Scuseria, MA Robb, et al., "G03 Rev. E.01," Gaussian, Pittsburgh, PA, USA, **2007**.
[70] JS Gómez-Jeria, "D-Cent-QSAR: A program to generate Local Atomic Reactivity Indices from Gaussian 03 log files. v. 1.0," Santiago, Chile, **2014**.
[71] Statsoft, "Statistica v. 8.0," 2300 East 14 th St. Tulsa, OK 74104, USA, **1984-2007**.